Late Quaternary deep-sea sedimentation in the western Black Sea: New insights from recent coring and seismic data in the deep basin

G. Lericolais[a, *], J. Bourget[b], I. Popescu[c], P. Jermannaud[d], T. Mulder[e], S. Jorry[a], N. Panin[c]

[a] IFREMER, Géosciences Marines, Centre de BREST, BP 70, F29200 Plouzané Cedex, France
[b] Centre for Petroleum Geoscience, School of Earth and Environment, The University of Western Australia, 35 Stirling Highway, Crawley, WA 6009, Australia
[c] GeoEcoMar, 23–25 Dimitrie Onciul Street, RO-024053 Bucharest, Romania
[d] BEICIP-FRANLAB, 232, Avenue Napoléon Bonaparte, P.O. Box 213, F 92502 Rueil-Malmaison, France
[e] UMR 5805 EPOC, OASU, Université Bordeaux 1, Avenue des Facultés, Cedex, Talence, F 33405, France

*: Corresponding author : G. Lericolais, fax: + 33 1 46 48 22 48 ; email address : gilles.lericolais@ifremer.fr

Abstract:

The Danube River Basin–Black Sea area represents a unique natural laboratory for studying the interplay between lithosphere and surface as well as source to sink relationships and their impact on global change. This paper addresses some information on the "active sink" of the system; i.e. the Danube deep sea fan and the Black Sea basin. The present study focuses on the distal sedimentary processes and the evolution of sedimentation since the Last Glacial Maximum. This is investigated through recently acquired long piston coring and shallow seismic data recovered at the boundary of influence of the distal part of the Danube turbidite system (to the north-west) and the Turkish margin (to the south). This dataset provides a good record of the recent changes in the sedimentary supply and climato-eustasy in the Black Sea region during the last 25 ka. This study demonstrates that the deep basin deposits bear the record of the Late Quaternary paleoenvironmental changes and that the western Black Sea constitutes an asymmetric subsident basin bordered by a northern passive margin with confined, mid-size, mud-rich turbidite systems mainly controlled by sea-level, and a southern turbidite ramp margin, tectonically active.

Highlights

► Oceanographic results from survey carried out in the western Black Sea are presented. ► The Danube fan distal part: the Black Sea main depositional feature is described. ► This study is on the morphology and gravity sedimentation in the Black Sea deep basin. ► Data were collected at the boundary between the Danube fan and the Turkish margin. ► The dataset provide a good record of sedimentary supply and climato-eustatic changes.

Keywords: Black Sea ; deep sea fan ; Danube turbidite system ; Turkish margin ; thick mud turbidites; sediment gravity flow ; sedimentation forcing ; active margin ; source-to-sink

Introduction

During the last decade, most of the work carried out in the Black Sea by geoscientists has focused on the Holocene marine invasion, with exception of the studies related to hydrocarbon exploration in the area (i.e. Aloisi et al., 1992; Jones and Simmons, 1997; i.e. Robinson, 1997; Robinson et al., 1996; Robinson et al., 1995). The Holocene marine invasion has been fully discussed and is still a matter of debates (Aksu et al., 2002a; Aksu et al., 2002b; Algan et al., 2001; Algan et al., 2002; Çagatay et al., 2000; Demirbag et al., 1999; Lericolais et al., 2009; Lericolais et al., 2010; Lericolais et al., 2011; Lericolais et al., 2007a; Lericolais et al., 2007b; Major et al., 2006; Major et al., 2002b; Myers et al., 2003; Ryan et al., 2003) since the flood hypothesis from Ryan and colleagues (Ryan et al., 1997). Positively, these recent studies have demonstrated that the Black Sea semi-enclosed basin constitutes one of the most interesting research zones for high-resolution paleoclimatological and paleoenvironnemental reconstructions. Since the DSDP drillings (Ross, 1978b; Ross and Neprochnov, 1978; Ross et al., 1978), the lithology and mineralogy of deep sediments from the Black Sea have been well studied (i.e. Bahr et al., 2006; Bahr et al., 2005; Bahr et al., 2008; Bahr et al., 2009; Degens and Ross, 1974; Giunta et al., 2007; Major et al., 2006; Major et al., 2002b; Ryan, 2007; Strechie et al., 2002). However, only a few recent studies have focused on the deep-water architecture and sedimentation in the western Black Sea basin, where the main depositional feature is the Danube deep-sea fan (Konyukhov, 1997; Popescu et al., 2006; Popescu et al., 2004; Popescu et al., 2001; Winguth et al., 2000; Wong et al., 1994; Wong et al., 1997).

Oceanographic surveys carried out in the Black Sea in 1998, 2002 and 2004 in the framework of French-Romanian joint project and the European ASSEMBLAGE project (EVK3-CT-2002-00090) have collected a large amount of data (Multibeam echosounder data, Chirp seismic, Kullenberg and Calypso cores). This new dataset has been examined into the light of three main objectives:

1. To study the nature of the deposits and the associated sedimentary processes in the deep western basin, at the limit of influence of the Danube turbidite system;

2. To understand the stratigraphical evolution of the sedimentary deposits in the deep western basin and their significance in terms of paleoenvironmental changes;

3. To provide a first assessment of the evolution and quantification of climate, tectonic and eustasy forcing on the sedimentation in the western Black Sea basin, along both southern and northern margins.

1. Regional settings

1.1 Hydrography and Physiography

The Black Sea is one of the largest anoxic basins in the world, with an area of 432 000 km^2. It represents a marginal basin connected to the external Mediterranean Sea over a sill located in the Bosporus Strait (Ross and Degens, 1974). Most of the rivers in Eastern and Central Europe drain into the Black Sea. The north-western part of the basin drains the largest Europeans rivers, the Danube (817,000 km2 of drainage basin), the Dniepr, the Dniestr and the Southern Bug. To the South, Anatolian rivers deliver more than 33% of the total sediment input into the Black Sea (Popescu, 2002), even if they represent only 8% of the total freshwater discharge.

Ross et al. (1978a) proposed that the Black Sea water level has independently oscillated from the global ocean, as it was an isolated basin for any water level below the depth of the strait (i.e. Dardanelles and/or Bosporus). Consequently, the high/low positions of the Black Sea level are more directly influenced by dry-wet cycles in Eurasia than eustatic cycles of the world ocean. During the Black Sea lowstands (i.e glacial times), the basin was isolated. The large freshwater inputs from the major rivers and the temporary absence of marine water input changed the Black Sea into a fresh (Soulet et al., 2010) to brackish lake. Presently, the hydrography of the Black Sea is characterised by the presence of a pycnocline between 100 and 200 m water depth separating a salty-near-surface water (~18 ‰) from a deep saline water (about 22,5 ‰) of Mediterranean origin that induces anoxic conditions below 150 mbsf (i.e. Bahr et al., 2005; i.e. Glenn and Arthur, 1985; Murray et al., 1989).

1.2 Geological settings

The opening of the Black Sea took place in a back-arc geodynamic regime, during Cenomanian to Coniacian times, due to the trench retreat of the Pontides subduction system (closing of the Tethyan Ocean northward; Robinson, 1997). The present Black Sea morphology has been determinate by the Mid-Cretaceous to Eocene extensional phase (Nikishin et al., 2003), followed by a final compressional dynamic (from late Eocene to recent times). The Black Sea is divided into two basins separated by the Andrusov ridge (Robinson, 1997): the western basin (underlain by oceanic to sub-oceanic crust) and the eastern basin (underlain by a continental crust of about 10 km thick). The western basin is filled by a 19 km thick sedimentary cover (Nikishin et al., 2003; Robinson, 1997). Five main seismic sedimentary units have been recognized in the whole basin, from the Upper Cretaceous to the Pliocene – Quaternary (Nikishin et al., 2003; Tugolesov et al., 1985). The latter consists of a 2,5 – 3 km thick, mostly represented by clayey sediments, deposited under a rapid Pliocene-Quaternary subsidence due to down-bending of the lithosphere in compression conditions (Nikishin et al., 2003). On the Turkish margin, the narrow shelf includes the offshore extension of the Western Pontides thrust belt. The large amount of erosion on the shelf and the presence of the thrust belt onshore suggest that numerous basin floor fans should be deposited throughout the post-rift sequence (Robinson, 1997).

The Turkish margin is marked by the presence of the North Anatolian Fault (N.A.F) southward (Fig. 1). The N.A.F is a right-lateral strike-slip fault zone, which extends about 1400 km from eastern Turkey to the Aegean Sea (Alpar and Yaltirak, 2002; Armijo et al., 1999; Armijo et al., 2002; Beck et al., 2007; Elmas, 2003; Faccenna et al., 2006; Flerit et al., 2004; McClusky et al., 2000). The North-Anatolian Fault is considered as a major active boundary between Anatolia and Eurasia plates. In north western Turkey, the westward displacement of the northern branch of the N.A.F (~20 mm per year; Facenna et al., 2006) induced an important seismic activity, marked by a set of recent high magnitude earthquakes (Barka et al., 2000; Beck et al., 2007; Pondard et al., 2007; Stein et al., 1997).

1.3 The Danube deep-sea fan

The Danube deep-sea fan (or turbidite system) is developed in the north-western part of the Black Sea, fed by sediments from the Danube (Popescu et al., 2004; Winguth et al., 2000), whereas the northern fan (Dniepr deep-sea fan) was fed by eastern rivers: the Dniepr, the Dniestr, and the Bug (Fig.1). Winguth et al. (2000) postulated that the Danube deep sea fan grew after the connexion of the Danube River with the Black Sea, at about 900 ka BP.

The same author recognized eight seismic sequences in both Danube and Dniepr fans, consisting of typical turbidite "fan" facies (e.g channel/levee systems, overbank sediments, mass transport deposits). Each of the eight sequences is separated by parallel and continuous reflectionsreflections interpreted as hemipelagic layers deposited during the sea level highstands (Interglacial periods). The last active complex grew during the last sea level lowstand in the Black Sea, i. e. the Last Glacial Period (Popescu et al., 2001; Winguth et al., 2000).

The most recent active fan extends about 150 km downslope of the shelf break, offshore the mouth of the Danube. The depositional system is connected to the slope and to the shelf break by the Viteaz canyon, which is a 2.5–4 km wide, V-shaped and northwest-southeast oriented system (Popescu et al., 2001). At about 800 m deep, the upper slope canyon evolves into a large single channel (Danube Channel, Fig. 2New), which is 2.4 km wide and 270 m deep (between the channel floor and the top of the levees). The levees are roughly asymmetrical (higher and wider right levee) and well developed, attesting to significant overbank deposition.

Numerous studies including Ryan et al. (1997), Major et al. (2002a; 2006; 2002b) or Lericolais et al. (2009; 2010; 2011; 2007a) have shown that the relative sea level at glacial times was between 100 and 150 m below the present day sea level. As consequence, the present day shelf of the north-western margin was exposed and the Danube mouth was directly connected to the Viteaz canyon head (Popescu et al., 2001; Winguth et al., 2000). Hyperpycnal flows are supposed to be responsible for the deposition of a large volume of sediments on the slope and the deep basin (Popescu et al., 2001).

1.4 The western Turkish margin

Only a few studies have focused on small parts of the central Turkish shelf (Duman et al., 2006), the Sakarya delta and submarine canyon (Algan et al., 2002), and off the Bosporus strait (Aksu et al., 2002b). In addition, Terikoglu et al. (2001) and Dondurur et al. (2009) have provided a description of the eastern Turkish margin morphology.

Sediments along the western Turkish margin (Fig. 1) are mainly transported by the two major rivers which are the Sakarya River (824 km long and 56 504 km^2 watershed) and Filyos River (228 km long and 13 156 km^2 watershed). The Turkish continental margin shows a very narrow shelf (locally < 7 km) and a steep continental slope (average from 5° to 9 °). The upper slope is incised by numerous canyons, down to the bathyal plain at about 1800 m deep (Duman et al., 2006). As our data do not cover the slope and shelf, we used the ETOPO 2 bathymetric charts for additional information along the western Turkish margin, updip our cores location. The data reveal an important canyon system offshore the Sakarya river and smaller canyons offshore Filyos river, where a fan development occur (Algan et al., 2002) (Fig. 1). The transition between the continental slope and the bathyal plain is marked by a very sharp change in slope. Previous studies of the western and the eastern basins mentioned flat-relief morphology and the absence of sedimentary bodies in the deep basin (Rotaru, 2010; Zonenshain and Pichon, 1986)

2. Materials and methods

2.1 Acoustic mapping

The bathymetry and acoustic imagery are provided by a multibeam echosounder (SIMRAD EM1000 and EM300) conducted on the R/V *Le Suroît* during the 1998 BlaSON and the 2000 BlaSON 2 cruises. Additional multibeam data (Thomson SEAFALCON 11) has been collected on the R/V *Marion Dufresne* during the 2004 ASSEMBLAGE1 cruise. Seismic lines were also collected during the BlaSON 1 & 2 cruises. The very high resolution source was a Chirp sonar single channel, with a frequency sweeping from 1.8 to 5.3 kHz.

2.2 Sedimentary cores

Kullenberg cores BLKS-9810 and BLKS-9822 were collected during the BlaSON 1 cruise while B2KS32 was collected during BlaSON 2 cruise (Table 1). Core BLKS-9810 was studied by Major et al. (2002a; 2002b). In addition, Calypso piston cores MD04-2762 and MD04-2789 were collected in the deep basin during the ASSEMBLAGE 1 cruise (Table 1). Physical properties of cores were logged on board with a Geotek Multisensor Core Logger (magnetic susceptibility and gamma density). Thin slabs of 15 mm thick were sampled on each cores and analysed with the SCOPIX X-ray image processing tool (Migeon et al., 1999). Subsamples were taken in order to obtain the carbonate content (using gasometrical calcimetry) and the grain size measurement (using a Malvern MASTERSIZER S). Sedimentary facies have been defined using: (1) photography, visual description, and x-ray imagery; (2) grain size analysis and CaCO3 content; (3) usual facies classification used in similar environments (Normark et al., 1997; Zaragosi et al., 2000).

2.3 Stratigraphy

The stratigraphic framework is based on AMS ^{14}C dating (performed at the Poznan Radiocarbon Laboratory, Poland, ETH Zurich and Artemis Gif sur Yvette) and regional lithostratigraphy analysis, according to previous paleoenvironnemental studies done in the Black Sea using marine sediments (Bahr et al., 2006; Bahr et al., 2005; Bahr et al., 2008; Jones and Gagnon, 1994; Lericolais et al., 2009;

Lericolais et al., 2010; Lericolais et al., 2011; Major et al., 2002a; Major et al., 2006; Major et al., 2002b; Popescu et al., 2001). The Black Sea reservoir age constitute an important problem to solve. Recently, Siani et al (2000) have proposed for the more recent period, a reservoir age of 415±90 years BP for the Black Sea, based on 6 collected shells from the Black Sea, the sea of Marmara and in the vicinity of the Bosporous. But, a reservoir age of about 1280 years was deduced from the occurrence of the Santorini Minoan ash in the Unit II of Jones and Gagnon (1994) of several south Black Sea cores recovered between 400 and 700 m below present sea level (Guichard et al., 1993). If we include documentation from Jones & Gagnon (1994), Bahr et al. (2005) Kwiecien et al. (2008) and Fontugne et al. (2009), then reservoir ages are extending from 400 to 1280 years. Recently, Soulet et al. (2011a) proposed a Black Sea "Lake" reservoir age evolution since the Last Glacial. From their studies, these authors proposed that the reservoir age prior to ~26 kyr BP were constant within an uncertainty of 155 ± 100 yr and increased after 26 kyr BP reaching values of ~2000 yr and ~1500 yr at around 23 kyr BP when deep and shallow water reservoir ages progressively decoupled. At 17.2 kyr BP, the reservoir age quickly dropped towards values of ~250 yr before the onset of the Bølling-Allerød (from ca 14.7 to 12.7 kyr BP) which is characterized by an instantaneous increase in the reservoir age of 500 yr, reaching ~750 yr. During the Younger Dryas, deep water reservoir ages increased to ~900 yr whereas shallow water reservoir ages displayed an opposite trend reaching stable values of ~280 from 13.8 kyr BP to the end of the Younger Dryas cold event. At the lacustrine to marine transition, the reservoir age was approximately 300 yr. From this work calendar ages can be approached by utilizing the most recent calibration curve (Reimer et al., 2009; Soulet et al., 2011a) through the program *Calib* version 6.0.1. (Stuiver and Reimer, 1993)

Except for the AMS ^{14}C dates obtained from organic matter, the AMS measurements and their calibrated age are resumed in Table 2. The correlation between all the studied cores has been established using radiocarbon dates, lithological boundaries, red layers (Bahr et al., 2005; Major et al., 2002b) and carbonate content evolution. All the cores correlate with the lithological units described by Ross and Degens (1974) and later by Giunta et al. (2007) in cores from the western Black Sea basin.

3. Results

3.1 Morphology

3.1.1 Lower Danube turbidite system (DTS)

The extended multibeam imagery cover allows the refining of the surface channel network distribution in the Danube Turbidite System (DTS). At least six channel-levee systems, named from (U0 to U6) can be identified (Fig. 2A) while fours systems were previously identified by Popescu et al. (2001) who did not have a complete multibeam DTM for their study. Each channel-levee system is connected to the main canyon – channel system (Viteaz canyon and Danube Channel; Fig. 2B), and seem to have been built through repeated avulsions (Fig. 2B). Indeed, Popescu et al. (2001) demonstrated that the DTS channel network results from repeated channel avulsions that occurred through the Quaternary. These authors showed that each channel-levee systems was characterized by seismic morphologies typically observed in mud-rich deep sea fans i. e. the Indus Fan (Clark et al., 1992; Kenyon et al., 1995), the Amazon Fan (Damuth et al., 1988; Flood and Damuth, 1987; Flood et al., 1994) and the Zaire Fan (Droz et al., 2003; Droz et al., 1996; Marsset et al., 2009; Savoye et al., 2000b). Channels are characterized by basal high amplitude reflection packages (HARPs), well-developed asymmetric levees, with onlap geometry between each levee of different units (Popescu et al., 2001).

On multibeam bathymetry, the Danube deep-sea channels are highly sinuous and associated with wide levees where sediment waves develop (Fig. 2B). Following the seismic analysis of Popescu et al (2001), these channel/levee systems have been numbered from 0 to 6 from older to younger (Fig. 2A). The size of each individual channel/levee unit decreases downstream and its bathymetric expression on the present-day sea-floor becomes less pronounced (Fig. 2B). In the bathyal plain (> 2100 m water depth) the main channels are diverging at distal avulsion points and feed a set of smaller distributary channels (Fig. 2A). These distal channels are associated with small-relief levees and upslope-migrating sediment waves are still recognized (Fig. 2B). Reflectivity map (Fig. 2A) in these distal area are characterized by patches of higher reflectivity inter-fingered with / or at the mouth of

the distributary channels. This is a classical feature of deep-sea fans typically associated with channel-lobe transition zones and distal lobes (Savoye et al., 2000a).

Reflectivity patterns at the mouth of the distributary channels do not always allow characterizing the lobe extension due to the relatively dense pattern of distributary channels. This complexity is often observed along mud-rich deep-sea fans (Jegou et al., 2008; Migeon et al., 2010; Savoye et al., 2000a) and would be related to the heterogeneity of the sediments deposited in these distal areas. Conversely, smaller, sand-rich fans usually show a single, well-defined high reflectivity lobe at the channel-mouth (Bourget et al., 2010; Gervais et al., 2001; Mas et al., 2010).

The distal termination of the U4 to U6 deep-water channels (corresponding to the younger channel/levee systems) are marked by numerous avulsion points, each sub-unit feeding a small, relative high-backscattering lobe (Fig. 2A), which are generally less than 7 km long and 4 km wide. The lack of well-defined reflectivity patterns in older channel/levee complexes (i.e. units U0 to U3, Fig. 2A) are also likely due to the deposition of hemipelagic sediments after their avulsion. For these older units (U0 to U3), the seismic lines acquired in the deep basin (Fig. 3 and 4) have been used to estimate the extension of the lobe deposits. The lobe morphology in the DTS appears to be mainly controlled by the morpho-structural context leading, at the system scale, to a progressive confining of the sedimentary deposits.

Indeed the distal terminations of the channel/levee systems U1 and U2 are confined against the system U3 which runs almost perpendicular to the slope (Fig. 2A). The channel/levee complex U3 is the best developed unit which overlies the older units and, extends down to the deep basin at about 2200 m of water depth (Fig. 2). The lobe complexes of the younger units U4 to U6 developed in a zone of decreasing accommodation, between the older units and the Dniepr turbidite system (Fig. 2A). This morphological development is probably induced by autocyclic processes (Popescu et al., 2001).

3.1.2 The bathyal plain

Downstream of the distal lobe, the multibeam bathymetry is characterized by the absence of geomorphological features on the sea-floor (Fig. 2B). Seismic reflection profiles in the area (Fig. 3 and

4) shows that this area consists of the distal termination of the Danube turbidite system in the deep basin inter-fingered with distal basin plain deposits. Three distinct seismic units are observed. The lowermost seismic unit (P1) consists of acoustically low amplitude to transparent, sub-horizontal continuous reflections (Fig. 3 and 4). This pattern is often associated with fine-grained distal turbidites (Winguth et al., 2000). The seismic unit P1 is overlain by a thick, chaotic to low amplitude, chaotic to bedded continuous reflections package (L2). Upward, relatively small channel-levees systems interpreted as a distal distributary channels are observed (Fig. 3 and 4). These channels are associated with the seismic unit L2 (Fig. 4). Based on the bathymetry data, these distributary channels belong to the channel/levee system (Fig. 2B). The seismic unit L2 is divided in three sub-units (L2-a, L2-b and L2-c; Fig. 3 and 4), interpreted as three individual depositional bodies. They display an overall retrogradational organization (Fig. 3 and 4) and correspond to lobe deposition from the DTS channel/levee U3 (Fig. 2A). More detailed observations show that each sub-unit displays a particular geometry:

(1) L2-a is a progradational sub-unit, mainly composed of chaotic to continuous bedded reflections of generally high amplitude. The unit downlaps P3 (Fig. 3 and 4).

(2) L2-b and L2-c are retrogradational sub-units showing chaotic to poor-continuous bedded reflections, where small-size filled channel-like features can be recognized (Fig. 3 and 4).

Seismic unit P3 onlaps L2 and shows the same acoustically pattern than P1 (i. e. sub-horizontal, low-amplitude to transparent echo-facies). In this unit, several echo-facies variations are recognized, although they could not be interpreted in terms of sub-units due to the lack of internal major unconformities. The sedimentary architecture of the basin plain in this area suggests that two sources of sediment are inter-fingering at 2200 m of water depth. A northern source is characterized by the stacking of > 50 ms thick (TWT) distal lobes showing a progradational to retrogradational stacking and is attributed to the channel/levee complex U3 (Fig. 2A); a southern source onlaps these lobes and is interpreted as thick distal deposits from the Turkish margin, out of the DTS influence (Fig. 3 and 4).

3.2 Sediment distribution

Three cores were collected in the outer fringe of the Danube Turbidite System (DTS) (MD0427-62, MD0427-89 and B2KS-32). One core (BLKS-9822) was collected on the Danube Turbidite System levee in between the sinusoidal distributary channel of the U3 distal lobes (Fig. 3). These four cores are described on figure 5. Core BLKS-9810 studied by Major et al. (2002a; 2002b) is presented here as a reference. Core information is presented in Table 1.

The uppermost hemipelagic unit of the deep basin cores (Unit 1 = D1) is a coccolith-bearing, light olive-gray, organic-rich and varve-laminated (Fig. 5). Unit 2 (D2) is a dark olive-grey sapropel (Fig. 5). Unit 1 (D1) and 2 (D2) attest to oxygen-depleted conditions of the Black Sea (i.e. high sea level after the last marine invasion). We further refine our stratigraphy using the well defined 2700 y BP Unit I/Unit II boundary (Jones and Gagnon, 1994). The base of the sapropel dated at 7540 y BP (Jones and Gagnon, 1994) is quite older than our AMS-14C dating at 7386 y BP (core MD04-2762, Fig. 5) and 7300 y BP (core BLKS-9822, Fig. 5).

The relative chronostratigraphy of the presented cores (Fig. 5) refer also to the evolution of the carbonate content. At least three of the four studied cores show a more-or-less distinct double peak in the carbonate content, localized between the base of the sapropel layer and the top of the reddish-brown muds (Fig. 5), as previously observed (Bahr et al., 2006; Bahr et al., 2005; Major et al., 2002a; Major et al., 2002b). Previous studies have shown that the age of reddish brown layers range between 18 to 15.9 ka BP cal (Major et al., 2006) corresponding to the end of the Last Glacial Maximum (LGM). Below these reddish-brown layers, all the cores show similar deposits (without significant carbonate content, lithofacies or colour changing) and return ages between 21 to 25 ky 14C BP. Even if these dates were obtained on organic matter, we can be confident in attributing this Unit to the Last Glacial period in concordance with Lericolais et al. (2011) where LGM organic matter dates were correlated with a Dreissena shell. This first observation is consistent with the previous results that indicated a relative stable sedimentary record during the LGM (Bahr et al., 2006; Bahr et al., 2005; Major et al., 2002a; Major et al., 2002b).

Photography, X-ray image, description and mean grain size analysis for cores MD04-2762 and MD04-2789 show that these cores are composed of more than 80 % of fine grained turbidites (Fig.6). The low percentage of hemipelagic deposits suggests deposition by muddy turbiditic flows and/or very low hemipelagic sedimentation rates. The average mean grain sizes on these cores range between 5 to 100 µm, suggesting that the sediments supplied from to the deep basin are dominated by very fine-grained material. Thick mud turbidites are the dominant facies in the cores, reaching thicknesses of about 50 cm (on MD04-2789; Fig. 6). They are characterized by fine sand to silt turbidite base generally showing planar lamination (rarely small current ripples) and normally graded , interpreted as Bouma facies Tc and Td (Bouma, 1962). The Tc/Td packages fine upwards to slightly normally to ungraded dark grey to brown mud layers, characterized by lack of bioturbation and microfossils and by the presence of oxidation patches and interpreted as Te facies (Bouma, 1962), resulting from the decantation of the turbidity current nepheloid cloud.

Upslope, the sedimentary deposits observed on the U3 levee (core BLKS98-22; Fig. 5) are dominated by thin-bedded turbidites (Fig. 5), similar to sedimentary facies associated with the overbank of turbidity currents along the levee flanks (Piper and Savoye, 1993). These deposits are characterized by rippled to parallel laminated fine sand to silts (Tc/Td), fining upwards to mud turbidites (Te) and hemipelagites. A similar facies is observed in core MD04-2762 (deep basin) located between 24.7 and 31 mbsf (Fig. 5 and 8). This level is dominated by fine grained turbidites with basal sandy layers fining and thinning upwards (Fig.6), interpreted as the result of the overbank of turbidites along the flanks of small-size distributary channels. This last interpretation is obtained by the study realized by Popescu et al. (2001). Considering the position of the core, at the boundary of influence between the Turkish margin and the Danube turbidite system, this thin-bedded turbidite could be the result of a short time interval of lobe deposition fed from the north by the channel/levee complex U3 (Fig. 2).

At the top of the three deep-basin cores, two particular sedimentary intervals were correlated (Fig. 7). Two thin *debrites* on MD04-2762 and B2KS-32 and two turbidites sequences with sapropel clasts in MD04-2789 overlie the first sapropel deposit. Each of them is separated by a thin (~10-20

cm) sapropel deposit, allowing the three cores to be correlated (Fig. 7). Above the sapropel-reworking sequences, cores MD04-2762, B2KS-32 and MD04-2789 (Fig. 5 and 7) record two thin (~20 to 90 cm thick) thick mud turbidites (H1 and H2 on Fig. 7), interbedded with thin (a few cm) Sapropel units (S, Fig. 7).

In core MD04-2762, disorganized clay with sapropel clasts can be interpreted as a debris flow deposit, in agreement with the classification from Mulder and Alexander (2001). In B2KS-32 (located at 6.5 km from MD04-2762), this facies forms thinner intervals (~20 centimetres each) and contains smaller clasts. This sedimentary record in the deep basin seems to correlate with two post-transgression mass-wasting events on the Turkish margin. The facies observed in the core MD04-2762 (Fig. 7) suggests an axial position of the debris flow deposit. The thinner *debrite* facies occurring laterally to core MD04-2762 may reflect the overspilling of the upper part of the flow. Core MD04-2789 is located at 17 km westward, on a ~19 metres local topographic high. The sapropel-reworking turbidites in this core may reflect the lateral transformation of the initial flow, from cohesive, matrix-supported, mixed sand and mud debris flow to a turbulent, fine-grained flow (Middleton and Hampton, 1973; Shanmugam, 2002).

Another facies observed in both cores from the deep basin (MD04-2762) and channel-levee complex (BLKS-9822) is characterized by turbidites with reddish clay in the thin-bedded turbidites of the U3 levee and in the thick, mud turbidites of MD04-2762 (Fig. 5). This facies is not observed in cores MD04-2789 and B2KS-32 due to the depth limitation in core recovery at those sites (Fig. 5). This reddish-brown facies is an important litho-stratigraphic marker in the Quaternary records of the Black Sea basin (Bahr et al., 2006; Bahr et al., 2005; Kwiecien et al., 2009; Major et al., 2006; Major et al., 2002b) and will be discussed in the following sections.

A special study has been carried out on core MD04-2762 as it has been recovered at 2210 m deep in the basin, at the boundary of the Danube Turbidite System and the Turkish margin (Fig. 1). Based on vertical facies and grain-size trends, five sedimentary intervals (lithozones) can be differentiated (Fig. 8):

- *Lithozone 1* is made up of hemipelagic coccolith-bearing, light olive-gray, organic-rich and varve-laminated clays at top and of dark olive-grey sapropel at the base;

- *Lithozone 2* consists of a few mm to 10 cm thick silt beds overlaid with homogenous clay laminaes. The basal silt layers have a sharp to smooth basal contact, rarely erosive, and are fining-up. They typically display horizontal laminae (rarely oblique-cross laminae) consisting of an alternance of silt and silty-clay. The upper part is characterized by the lack of sedimentary structures and of bioturbation and is poorly graded;

- *Lithozone 3* is characterized by thick very-fine sand to silt overlaid with 20 to 110 cm of poor to ungraded clay. The basal layer is coarser and has a sharp to smooth basal contact, rarely erosive, and is normally-graded. This lithozone presents reddish brown fine grained clays without neither structure nor grain size trend;

-. *Lithozone 4* is a particular sedimentary interval presenting superposition of very fine sand with clay layers. The basal contact is sharp or erosive and constitutes the coarser part of the lithozone which represents more than 70 % of the total facies. This base is massive and lacks of structure;

- *Lithozone 5* consists of thick muddy turbidites presenting horizontal laminae (rarely oblique-cross laminae) made in alternance of silt and silty-clay. These turbidites are interbedded with thin hemipelagic deposits of fine grey to light brown bioturbated clays, showing no internal structures or grain size trend.

3.3 Correlation of core MD04-2762 with B2Ch-135 seismic line

The synthetic log of the MD04-2762 core differentiated in *lithozones* has been correlated with the three main seismic units identified on Chirp seismic line (Fig. 4 and 8).

Seismic units P1 (*variable amplitude, continuous* reflections) and L2 (*medium amplitude, poor continuous* to *chaotic* reflections) seem to correspond respectively to the *lithozones 5* (thick mud turbidites) and *4* (lobes deposits originated from the channel/levee system U3) on the core (Fig. 4 and 8). The upper intervals (*lithozones 1* to *3*), all consisting of thick mud turbidites, are correlated to the

seismic unit P3. Following our age model, P1 and L2 (*lithozones 5 and 4*) correspond to LGM deposits, whereas P3 (*lithozones 1 to 3*) includes deglacial to most recent deposits (Fig. 4 and 8), which are onlaping the DTS distal lobes.

Core MD04-2762 links the morphological units observed on the seismic line with sedimentary facies. In this portion of the deep basin, the progradation of lobe deposits from the Danube Turbidite System during the LGM (Popescu et al., 2001) (Fig. 4 and 8) is followed by the progressive retreat of the lobe deposits (retrogradation of the seismic units L2b and L2c probably following upstream channel migration or avulsion; Fig. 4). From previous work (Popescu et al., 2001; Winguth et al., 2000), it is clearly confirmed that no sediment from the Danube system is provided to the deep basin after 14 ka and therefore onlaping distal deposits are interpreted as being sourced from the Turkish margin which dominates the sedimentary record during the deglacial and Holocene times (Fig. 8).

4. Discussion

4.1 Evidence for earthquake-induced, unchannelized gravity currents sourced from the Turkish margin

The sedimentary units P1 and P3 (i. e. deposits originated from the Turkish margin for P3) consist mainly (> 80%) of thick mud turbidites associated with thick transparent units visible on the chirp profiles (Fig. 4). Such sequences showing thick structureless homogeneous "Te" muds have already been described along deep basin plains such as in the Mediterranean (Kastens and Cita, 1981; Rothwell et al., 2000; Stanley, 1983), the NW African basin (Wynn and Stow, 2002), and the Oman basin (Bourget et al., 2011). Presences of transitional sandy-muddy and muddy debrites are common in distal fan settings and are often transitional and therefore related to underlying turbidites (Hickson, and Lowe, 2002). These deposits are usually resulting from poorly channelized to unchannelized, large volume turbidity currents (Bourget et al., 2011; Wynn and Stow, 2002). Some authors proposed that the unusual thickness of the muddy "Te" could result from several, successive surges occurring in a voluminous, mud-rich turbidity current rather a discrete gravity flow (Lowe, 1982; Tripsanas et al., 2004; Wynn and Stow, 2002). A possible explanation is that these thick muddy turbidite deposits

would be due to successive mass-wasting along the continental slope (Bourget et al., 2010; Wynn and Stow, 2002). In the Makran (a semi-desert coastal strip along the coast of the Arabian Sea and the Gulf of Oman) active margin, these processes and the thick distal deposits that they produce have been linked to major earthquakes (Bourget et al., 2010).

The Turkish margin is bordered by the highly active North Anatolian Fault (Fig. 1). Previous studies in the Eastern Black Sea have shown that the activity of the North Anatolian fault is also evidenced offshore (Cifci et al., 2003; Dondurur and Cifci, 2007; Rangin et al., 2002) and suggested a minor impact of the N.A.F. on the triggering of mass wasting processes along the continental slope based on the relative size of the slide scars. Inversely the observations of a dense distribution of slump-scars along the margin (Cifci et al., 2003; Dondurur and Cifci, 2009) support the hypothesis that submarine landslides as an important mechanism for triggering turbiditic flows. Recent earthquake distribution from USGS (http://earthquake.usgs.gov/earthquakes/world/turkey/density.php) shows that a portion of the Turkish margin located upward of our cores is particularly active. Earthquakes could generate the destabilize small portions of the shelf-edge and continental slope and form repeated mass-wasting events, possibly generating successive tsunamis waves and gravity flows (Bourget et al., 2011; Bourget et al., 2010; Talling et al., 2007; Wynn and Stow, 2002). Several historic tsunamis have been reported along the Black Sea Turkish coast (Altinok et al., 2011; Pelinovsky, 1999), and have been triggered by the activity of the North Anatolian strike slip fault (Fig. 1). Conversely the thick-mud turbidites observed in the deep basin plain could correspond to the "homogenites" studied by Kastens and Cita (1981) and (1984) or the "unifites" of Stanley (1983). Reeder et al. (1998) restrict the term "homogenite" to deposits having an homogeneous nature and related to the expression of a unique event with a definite stratigraphic position (Cita et al., 1996). Such "homogenites" have also been described in deep basins of Marmara Sea (Beck et al., 2007) or as the LGM Black Sea, in lakes (Chapron et al., 2006; Chapron et al., 1999). Cita et al. (1996) proposed that after a tsunami, resuspended sediments form a turbulent particle cloud that settled out gradually. In the Marmara Sea as well as in lake environments, such homogeneous deposits have been attributed to "seiche" effect (i. e. lake water oscillation in response to earthquake-induced mass wasting

processes). The water column oscillation is generally related to seismic activity (Cita et al., 1984), directly (by direct seismic wave propagation) or indirectly (earthquake induced mass wasting processes such as slides or slumps). If "seiche" effects are commonly generated in confined basin such as lakes or the enclosed Marmara Sea (Beck et al., 2007), the Black Sea basin, which extends on 432,000 km^2, appears to be a wide undergo "seiche" wave generation.

Previous work (Popescu, et al. 2001; Winguth et al., 2000) clearly concluded that the northwestern rivers stop providing sediments to either the Danube deep sea fan and to the Dniepr-Dniestr deep sea fan after the LGM. From the dates obtained in the studied cores, informing we can hat P3 was deposited after LGM although the Danube sediments were not reaching the deep basin. Therefore, we can conclude that the thick mud turbidites observed in the deep basin sediments, especially for P3, are sourced from the Turkish margin and are the result of synchronous mass-wasting events along the slope, such as observed along the Makran (coast of the Arabian Sea and the Gulf of Oman) active margin (Bourget et al., 2011; Bourget et al., 2010). Such events could be generated during earthquakes related to the N.A.F activity.

The nature of the distal deposits and the unusual amount of mud in the turbidites are also likely related to the physiography of the margin. Indeed the loss in flow velocity induced by the sharp change in gradient at the break of slope and the very low slope gradient ($< 0,1$ °) in the basin plain lead to rapid deposition of coarser sediments, with only the finer-grained portion of the initial sediment load being transported to the basin. In addition, abrupt break of slope such as the one observed along the Turkish margin can limit the downslope formation of submarine channel and thus enhance the generation of unchannelized gravity currents in the basin plain (Bourget et al., 2011). The general low-amplitude and acoustically "transparent" echo-facies observed in the sediments sourced from the Turkish margin (Fig. 4) are typically thick, mud-rich turbidites (Beck et al., 2007; Chapron et al., 1999; Cita et al., 1996; McHugh et al., 2006). The thickness of the clayey layers finally requires an abundant source of fine-grained sediments in the catchment area and shelf (Bourget et al., 2010), which is the case along the Turkish shelf (Duman et al., 2006).

As after the LGM, it is known that the Danube deep sea fan does not receive any sediment from the northwestern rivers and according to the regional seismic activity, it comes that earthquakes may be the more common initial triggering mechanism of the mass-wasting inducing thick mud turbidites constituting P3 sequence, at least on this portion of the Turkish margin. Off the major Anatolian rivers, i. e. off the Sakarya and Filyos, rivers, a small-size fan development may occur in the proximal part (e.g. Algan et al., 2002; Dondurur and Cifci, 2007), possibly built by recurrent hyperpycnal currents (that could exit in the semi-freshwater Black Sea during sea level low-stand). Sediment overloading on the steep slope or gas hydrates (classically observed onto the Turkish shelf; Cifci, 2003) constitute additional triggering mechanisms which would explain the occurrence of typical distal turbidites also recovered in our cores.

4.2 Sedimentary record evolution in the deep basin

Both the location of the core MD04-2762 (at the boundary of influence of both the Danube Turbidite System and the Turkish margin) and its length (47 m) provide an outstanding record of the sediment supply evolution in the deep western Black Sea basin since the LGM. Most of the observed variations in the deep basin can be correlated with those recorded on the Romanian shelf (Bahr et al., 2005; Lericolais et al., 2010; Lericolais et al., 2011; Major et al., 2006; Major et al., 2002b).

4.2.1 The Last Glacial Maximum (~ 25 – 18 ka BP)

The LGM deposits consist of thick mud turbidites overlain by lobe deposits from the Danube Turbidite System.. Popescu et al. (2001) concluded that the youngest channel-levee system on the Danube deep-sea fan developed during the Neoeuxinian lowstand (Stage 2) in a semi-freshwater basin with a water level at least 100 m lower than that of today. Sediments supplied by the Danube were transported over the narrow shelf to the deep basin through the Viteaz canyon, which was directly connected to the leveed channel of this system. So, the progradation of the DTS at more than 2200 m of water depth is linked to an important sediment supply from the Danube River in relative low lake level connected to the Viteaz Canyon (Popescu et al., 2001). In this environment, it has been clearly

demonstrated by these authors and by Winguth et al. (2000) that a definite relationship exist between water level and Danube fan sedimentation: when water level is close to the shelfbreak during lowstands, fluvial sediments are transported to the deep-sea fan, while fan construction is essentially interrupted during water level highstands.

More, the channel/levee complex U3 was active during this period. Multiproxy records in LGM sediments from the Black Sea (Bahr et al., 2005; Major et al., 2006; Major et al., 2002b) also suggest that the LGM was characterized by stable climatic conditions.

4.2.2 Deglacial Times (~ 18 to 15.5 ka BP)

Immediately above the lobe deposits, the occurrence of very thick turbidite deposits associated with coarser grained turbidites and reddish-brown reworked clays (top of the *lithozone* 3) suggests enhanced sediment supply in the deep basin,. Although uncertainties in our age model (insufficient radiocarbon dating) do not allow a precise determination of the age of the sediment supply, it lies above LGM deposits and is directly overlain by carbonate-rich sediments. These carbonate-rich sediments have been dated by several authors as Bolling-Allerod deposits (Bahr et al., 2005; Major et al., 2006; Major et al., 2002b). On the north-western shelf, the reddish-brown layers have been dated from ~ 18.3 to ~15.9 ky BP (Major et al., 2006), in several pulses. Recently, four red layers interval were identified and dated by Soulet et al. (2011b) from 17.2 to 14.8 ka BP cal. From isotopic and geochemical proxies, several authors argued that their deposition was linked to a major melting phase of European ice (Denton et al., 2010) in response of the climate warming, ~3 ka before the Bolling-Allerod period (Major et al., 2006), drained by the north-western Danube and Dniepr rivers.

The red clays observed in core MD04-2762 must be carefully interpreted, as they consist of reworked material. However, the occurrence of reddish-brown layers in the sediment associated with coarse-grained thick reworking sequences (Fig. 8) provide new evidences that an unusually high deglacial sediment load has been brought into the Black Sea during this period. Core MD04-2762 is located in the deep part of the Black Sea basin but in the near vicinity of the Turkish margin. As these reddish clays has not been reported in the distal part of the Danube deep sea fan (Popescu et al., 2001;

Winguth et al., 2000), it is difficult to support a direct northern source for the red layers (Major et al., 2002a) associated to the European meltwater event. To explain the presence of these clays in this distal core, one can 'hypothesizethat they have been transported to the Turkish shelf and slope by strong surface currents such as the present day "rim current" gyre (Bahr et al., 2005). Intense dense water discharge into the Black Sea may have formed important turbid sedimentary plumes, easily transported along the western coast. But, a more local (southern) provenance may be attributed to an intensified weathering during deglacial times, which classically form red-coloured clays in Anatolia (Atalay, 1996). Whether the reddish-brown mud observed in the deep basin are sourced from the north-western or Anatolian Black Sea rivers, they must lie in the change in river sedimentary load (Major et al., 2006) linked to a major melting phase of European ice. This phenomenon can be recorded in the whole western Black Sea basin. We correlate the thicker coarser grained turbidite sequences of the *lithosome 3* to the Late Glacial warming that led also to the early melting of Anatolian glaciers (Akçar et al., 2009; Zahno et al., 2010), beginning at around ~ 18,3 ka BP. This implies a slight increase in the sediment supply onto the Turkish margin, and enhanced sediment failures and transport to the deep basin. The water brought to the Black Sea after this meltwater pulse event led to a rise of the Black Sea level to -40 / -20 m (Lericolais et al., 2009; Lericolais et al., 2010; Lericolais et al., 2011).

4.2.3 From Bolling-Allerod period to first sapropel deposition (~ 15,9 – 7,5 ky BP).

The observation of carbonate-rich sediments (i. e. *lithozone* 4) are consistent with those described in the cores recovered from the north-western Black Sea shelf and slope (Bahr et al., 2005; Giunta et al., 2007; Major et al., 2002b; Soulet et al., 2011a; Strechie et al., 2002). They have been attributed to inorganic carbonate precipitation due to hypersaturation of surface waters, linked to a reversing water balance of the Black Sea basin following the meltwater-driven highstand period (Major et al., 2006). Numerous studies have shown that the Black Sea experienced a lake level that reached ~ 100 m below present level during this period (Demirbag et al., 1999; Gorur et al., 2001; Lericolais et al., 2010; Lericolais et al., 2011; Ryan et al., 2003). However, the dating of this lake level is today uncertain and has been attributed at the Younger Dryas cold and dry event (beginning at ~

13,5 ka BP), which has reduced the river input in the Black Sea (Lericolais et al., 2007b). Using geochemical proxies from the north-western Black Sea sediments Major et al. (2006) propose that this lowstand period occurs during the warmer Bolling-Allerod and Preboreal ages (i. e. during the carbonate-rich sediments deposition), whereas the sea level may have risen through the Younger Dryas event (due to a lower evaporation rate under cold an arid climate). For Giosan et al. (2009), the level of the Black Sea has leveled down not more than -40 m. In each case, the carbonate-rich sediments recovered traduce the global sea level lowstand prior to first occurrence of sapropel deposition.

4.2.4 Onset of anoxic conditions (first Sapropel deposition) and post-transgression debrites.

All the cores used in this study record the onset of sapropel deposition (i. e. anoxic conditions). Major et al. (2006) showed that marine influence on Black Sea water chemistry began at ~ 9.4 ka BP, pointing to a Bosporus sill depth of - 30m below modern sea level at the time of reconnection. This was recently corrected by Soulet et al. (2011a) giving an age of 9 ka BP for the reconnection with a sill depth of -25 m. Thus, the date of ~ 7.4 ka BP obtained at the base of the first sapropel deposit does not coincide to the marine incursion itself, but corresponds to the time when salinity rose to a sufficient threshold for the depletion of bottom water oxygen required for sapropel formation (Major et al., 2006; 2011), calculated to be around 900 yrs by Soulet et al. (2011a).

Recent studies have shown that the rising of the lake level was high enough to cause erosion of the lowstand shoreline and upper slope (Giosan, 2009; Giosan et al., 2006; Lericolais et al., 2009; Lericolais et al., 2010; Lericolais et al., 2011; Ryan et al., 2003). Bahr et al. (2005) also recorded a peak in clastic input associated with an increase in grain-size on the western shelf sediments (Major et al., 2002b), suggesting an abrupt reworking event during marine transgression. The debris flow sequences (Fig. 7), the abundance (> 80 %) of large sapropel clasts (forming under -130 to 180 m depth in the Black Sea) suggests that the mass wasting events formed into the outer shelf or into the slope, as the debris flows commonly display poor erosive characteristics, due to hydroplaning (Mulder and Alexander, 2001). The two debrites/sapropel-reworking turbidites have been correlated in the

three cores, representing at least 23 km wide deposits in the deep basin. The relative thinness of the debrites may be due to their distal position (~ 250 km from the mouth of the Danube Delta and ~50 km from the shelf of Turkey).

Following the 7210 [14]C y BP datum obtained at the base of the first sapropel deposits in the Black Sea (core MD04-2762), and an averaging 10 cm/1000 years of hemipelagic sediment deposition for the Holocene obtained by Ross and Degens (1974) in the deep basin, we can conclude that these two intervals are contemporaneous to ~ 6 to 4 ky BP (Fig. 8). Considering that mass transport deposits have been often associated to Plio-Quaternary sea level lowstand (Bouma et al., 1989; Maslin et al., 2005; Nisbet and Piper, 1998), these mid-Holocene debris flows appear as an anomaly recorded in the distal basin, in respect with the continuous record of gravity processes on MD04-2762 since the LGM. They occurred during sea level highstand conditions, suggesting that they might not be triggered directly by gas-hydrate release, as the increase in hydrostatic pressure would have stabilized the hydrate deposits (Maslin et al., 2005). Major earthquakes could have been another possible triggering mechanism.

In the Amazon Fan, Maslin et al. (2005) identified mass wasting events linked to a sea level rise during deglacial times (~13 ka BP). In that case, the redistribution and/or enhanced sediment supply onto the shelf led to an abrupt overloading, which generates shelf-edge/upper slope instabilities (Bourget et al., 2010). Mass transport deposits have also been observed in the Nile Fan under sea level rise and linked to enhanced pluvial conditions and sediment purge (Ducassou et al., 2007; Garziglia et al., 2007).

The Holocene Climatic Optimum (HCO) (Berger and Loutre, 2002) has been recorded in the sediments from the Lake Van in eastern Anatolia between – 6.2 to – 4 ka BP (Wick et al., 2003) with the maximum extension of the forest-steppe under a wetter and possibly warmer climate (Landmann et al., 1996). Similar indications of humid transition have been reported in Western Europe and North Africa (Gasse and Fontes, 1992). Such a drastic change to more pluvial conditions may have induced the purge of the shelf and shelf-edge sediments accumulated during Bolling to Preboreal Black Sea

lowstand. The change in sedimentary dynamics after the marine invasion is illustrated by the end of activity of the DTS and the rapid progradation of the Danube delta (Popescu et al., 2001). Such enhanced sediment supply and/or relocation of the sediment deposition may have caused overloading on the steep Turkish continental slope. Increasing sediment failure during times of sea level rise has already been linked to the combination of loading by drowning of un-consolidated or poor-consolidated sediments deposited on tectonically active margins (Lykousis et al., 2007; Trincardi et al., 2007). Previous cited studies have shown that failures result from a combined forcing, where earthquakes are often final triggers in addition to pre-conditioning, climatically-driven factors (Canals et al., 2004).

The two debrites sequences observed in the western Black Sea Basin are possibly linked with the onset of the Holocene Climatic Optimum after ~ 6 ka BP. During this period, the combination of climatic, geotechnical, and seismic forcing may have led to optimal conditions for anomalous sediment failures. Additional radiocarbon dating of cores recovered in the deep basin, knowledge of the reservoir effect correction on the organic matter of the Black Sea as well as seismic data onto the slope and shelf are needed to obtain accurate timing, extension, and cause and process characterization of these mid-Holocene debris flows.

4.2.5 Middle Holocene to recent times.

The two thin (~20 to 90 cm thick) thick mud turbidites (H1 and H2 in cores MD02 2762, B2KS-32 and MD04-2789; Fig. 7) recorded above the sapropel-reworking sequences and interbedded with thin (a few cm) sapropel units (S, Fig. 7) suggest that the sediment supply from the Turkish margin has remained active even during the sea level highstand. These Holocene deposits are mainly composed of silt and clay, and may indicate the progradation of deltas off the main Anatolian rivers after the transgression. This is coherent in process with a post transgression age of the Sakarya delta (Algan et al., 2002) and even if this delta is quite far from the studied area, the main process encountered on the Turkish side remained the same.

4.3 Quantification of climatic, eustatic and tectonic forcing on the gravity sedimentation in the western Black Sea basin.

The last concordant sequence is onlaping the distal deposits of the Danube Turbidite System at 2200 m of water depth. During glacial times, the gravity sedimentation from the Turkish margin appears to be controlled by both regional tectonics and climatic forcing (i.e. enhanced sediment supply during deglacial and unusual wet periods). At a smaller scale, past work in the area has shown that the sediment supplied onto the shelf is controlled by climate at Eastern Mediterranean (Lamy et al., 2006). Due to their very short source-to-sink sediment transport route, active margins are indeed more likely to be influenced by high-frequency climate changes and the later are likely to be recorded even in the distal most turbidite deposits (Bourget et al., 2010). Tectonics, sea-level and climate changes are actively influencing the transfer of sediments along active margins and equally influence the stratigraphic architecture of the turbidite system at relatively short time-scales (< 100 ka).

Conversely, the north-western margin shows the development of medium-size, mud-rich turbidite systems (i. e. the Danube and Dniepr deep sea fans). Here the sediments are transported to the deep basin from a point source. The flows are channelized, confined (Winguth et al., 2000), typically depleted in fine sediments along the slope and in the bathyal plain until they reach lobe deposition at their most distal part. During the LGM, the Black Sea was a lowstand lacustrine body and the Danube deep sea fan was functioning. The direct connexion between rivers and canyons suggest a climate driven sedimentation at high resolution along the north-western shelf (Kwiecien et al., 2009). However at the scale of the Late Quaternary, the Danube Turbidite System activity is mainly control by lake level fluctuationsand is inactive during the Holocene when a large delta progrades at the river mouth onto a wide shelf (Popescu et al., 2004; Popescu et al., 2001). In general, our results illustrate the multi-scale forcing variability on the western Black Sea sedimentation, from the north-western passive margin controlled by lake level fluctuationsand glacial cycles, to the south-western margin on which tectonics shaped a typical ramp system and actively control the source-to-sink sedimentation.

Conclusion

Our study focuses on the deep-water architecture of the western Black Sea deep basin and its sedimentological characteristics. The Late Quaternary Danube turbidite system (to the North) displays a well-constructed morphology, underlined by at least six channel-levee systems associated with distal lobe complexes, reaching the 2200 m isobaths. The adjacent deposits, onlaping the Danube Turbidite System distal lobes in the deep basin, show a linear, drape-like morphology, represented by thick continuous reflections on seismic profiles. They generally consist of distal turbidite deposits supplied from the Turkish margin. Most of these turbidite sequences show a thick upper unit composed by homogeneous clastic clays, thus forming thick mud turbidites. Following previous work in similar basin settings, we interpret these facies to result from large volume unchannelized turbidity currents generated by successive mass-wasting events. The abrupt break of slope at the bathyal plain transition enhances the rapid deposition of coarse-grained material and limits channel development in the bathyal plain. We relate the origin of these deposits with the very high seismic activity of the North Anatolian Fault on the Turkish margin.

Our study is based on data at the boundary of influence of the Danube Turbidite System and the Turkish margin, and provides a new record of the changes in sedimentary supply, climate and sea level that occurred in the Black Sea region since the last ~ 25 ka. We demonstrated that the deep basin deposits bear the record of the Late Quaternary paleoenvironmental changes. The Last Glacial Maximum Period (~25 to 18 ka BP) was characterized by an important and relatively stable sediment supply with sediment transferred to the deep basin from both the northern Danube Turbidite System and the southern Turkish margin. The relative stable LGM period was followed by an increase of sediment transport to the deep basin, which is locally illustrated by progradation of lobe deposits from the Danube turbidite system in the deep basin, downlaping the Turkish deposits. Deposition of reddish-brown muds in the deep basin sediments is synchronous with similar deposits previously observed along the Romanian shelf and slope and are possibly linked to the melt of Eurasian ice sheets and Alpine glaciers by ~ 15 ky BP. Influx of meltwater to the Black Sea resulted in a early highstand sea level. The following Bolling-Allerod Preboreal warm period and the Younger Dryas cold event

have experienced alternative sea level lowstands and highstands that are not clearly underlain in the deep basin sediments. The onset of sea-level highstand after the Holocene marine invasion (~ 9 kyr BP) induced the end of the activity of the Danube Turbidite System whereas the gravity supply from the Turkish margin remained active throughout the Holocene.

We conclude that the western Black Sea basin constitute an asymmetric subsident basin bordered by a northern passive margin with confined mid-size, mud-rich turbidite systems, and a southern turbidite ramp built in a tectonically active margin setting.

Acknowledgements

Figure captions:

Fig.1: Location map of the study area, showing extension of the two main sedimentary features in the Western Black Sea Basin (WBSB) i. e. the Danube Turbidite System (DTS) and the Dniepr Turbidite System (after Popescu et al., 2001; after Wong et al., 1997); Bathymetry contours are from 50 m interval (source : ETOPO2); locations of the four sedimentary cores (red circles) and the 3,5 kHz seismic line (solid line); location of the possible sediment source for the portion of the deep basin studied, out of the DTS influence (red dashed line and arrows); location of the North Anatolian Fault (N.A.F). Bathymetric font modified from H. Gillet (2007).

Fig. 2: Multibeam reflectivity (A) and bathymetry (B) maps from the BlaSON1, BlaSON2 and ASSEMBLAGE1 cruises. Superimposed on the reflectivity map is the detailed interpreted morphology (Channel units U0 to U6; Complex Lobe U3: CL-U3) of the distal termination of the DTS (2200 m) and the deep basin, the location of the cores BLKS-9822, MD04-2762, MD04-2789 and B2KS-32, and the position of the seismic lines B2Ch 132, B2Ch 135 and B2Ch-136. Core BLKS-9810 has been published by Major et al. (2002a; 2002b).

Fig. 3: Chirp seismic profile B2ch-132 and B2ch-136 with core location for BLKS-9822 and B2KS 32. Seismic units P1 and P3 are associated with fine-grained distal turbidites. Unit L2 corresponds to a chaotic to bedded continuous reflections package. L2-a, L2-b and L2-c are three sub-units of L2 corresponding to three individual depositional bodies.

Fig. 4: Chirp seismic profile B2ch-135 and interpretation. Seismic units P1 and P3 are associated with fine-grained distal turbidites. Unit L2 corresponds to a chaotic to bedded continuous reflections package. L2-a, L2-b and L2-c are three sub-units of L2 corresponding to three individual depositional bodies.

Fig. 5: Correlation of the four studied cores based on lithologic units boundaries and AMS dates. Units D1, D2 and D3 correspond to the lithological units described by Ross and Degens (1974) and later by Giunta et al. (2007). The sapropel, the reddish-brown and the carbonate rich layers are the ones described by Major et al. (2002a; 2002b) and Bahr et al. (2006; 2005)

Fig. 6: Photography, X-ray image, description and mean grain size analysis for:

A) Thick mud turbidite sequence in core MD04-2789, with a basal fining-upward sequence formed by the deposits of suspended particles within turbidite surge overlain by a thick clayey, homogeneous, "Te" term (decantation);

B) Fining and thinning-up sequences in core MD04-2762 formed by the overbank of turbidity currents over small-size, lobe complex distributary channels.

Fig. 7: schematic representation of the two successive sapropel-reworking sequences observed and correlated between the three cores recovered in the deep basin, out of the Danube Turbidite System influence (i.e. B2KS-32, MD04-2762 et MD04-2789).

Fig. 8: Time scale of core MD04-2762 (deep basin): (a) lithologic schematic log and associated lithozones, seismic units (P1, L and P3), mean grain size (D50, μm), carbonate content (%), and (b) comparison with the carbonate content of the BlaSON1 core BLKS-9810 recovered onto the Romanian shelf (Major et al., 2002b); (c) the world sea level curve following Shackleton et al. (1987) and the GRIP $\delta180$ record (‰), compared with (d) Black Sea level curves plotted after Major et al. (2006, red dashed line) and Lericolais et al. (2009, black continuous line) tacking into account of a ~ 9 ky BP marine invasion (Soulet et al., 2011a); (e) Proposed sedimentary transfer scheme from the north and south-western margins to the deep Black Sea basin, from the last Glacial to recent times, following our preliminary results (Turkish margin) and previous studies (Popescu et al., 2004; Popescu et al., 2001; Winguth et al., 2000).

Black arrows indicate AMS 14C dating given in uncorrected age (Table 2). HCO for Holocene Climatic Optimum.

*Uncorrected age, uncertainty is presented in Table 2

*Uncorrected age, uncertainty is presented in Table 2

Core number	Latitude	Longitude	Depth (m)	Length (m)	Cruise	Year	Institute
BLKS-9810	44° 04.04' N	30° 50.68' E	378	7.71	BlaSON 1	1998	IFREMER
BLKS-9822	43° 02.27' N	32° 07.49' N	2100	7.17	BlaSON 1	1998	IFREMER
B2KS-32	42° 42.11' N	32° 46.71' E	2177	8.08	BlaSON 2	2000	IFREMER
MD04-2762	42° 38.89' N	31° 46.71' E	2210	47.3	ASSEMBLAGE 1	2004	IPEV - IFREMER
MD04-2789	42° 30.30' N	32° 31.00' E	2191	6.75	ASSEMBLAGE 1	2004	IPEV - IFREMER

Table 1: Core number, latitude, longitude, water depth and cruise details of cores investigated.

BLKS-98xx: cores recovered during BlaSON 1 cruise (1998)

B2KS-xx: cores recovered during BlaSON 2 cruise (2002)

MD04-: cores recovered during ASSEMBLAGE 1 cruise (2004)

Core number	Depth (cmbsf)	Conventional age ^{14}C BP	Calendar age cal. BP	Species analysed	# lab number
BLKS-9810	94,5	10640 +/- 80	12,123 ± 214	*TurriCaspia Caspia*	ETH-23298
BLKS-9810	118,5	11410 +/- 110	12,984 ± 103	*Dreissena Rostriformis*	ETH-23299
BLKS-9810	154,5	12790 +/- 110	14,142 ± 150	*Dreissena Rostriformis*	ETH-23300
BLKS-9810	186,5	12820 +/- 100	14,890 ± 159	*Dreissena Rostriformis*	ETH-23301
BLKS-9810	704	17760 +/- 130	20275 +/- 250	*Dreissena Rostriformis*	ETH-23302
BLKS-9822	4.5	2600 +/- 60	Not applicable	*Organic matter*	GIF-101540
BLKS-9822	23.5	7000 +/- 80	Not applicable	*Organic matter*	GIF-101541
BLKS-9822	26.5	7600 +/- 90	Not applicable	*Organic matter*	GIF-101542
BLKS-9822	90	18420 +/- 160	Not applicable	*Organic matter*.	GIF-102101
BLKS-9822	229,5	24000 +/- 220	Not applicable	*Organic matter*.	GIF-101543
BLKS-9822	328.5	25680 +/- 270	Not applicable	*Organic matter*	GIF-101544
BLKS-9822	711,5	24280 +/- 250	Not applicable	*Organic matter*	Lawrence Livermore Nat. Lab.
MD04-2762	31	2700 +/- 35	Not applicable	*Organic matter*	SAC-5878
MD04-2762	486	7210 +/- 50	Not applicable	*Organic matter*	POZ-13839
MD04-2762	4137,5	21820 +/- 150	Not applicable	*Organic matter*	POZ-17151

Table 2: AMS ^{14}C ages with calendar correspondences (Calib 6.0.1), using Soulet et al. (2011a) correction before calibration.
BLKS-98xx: cores recovered during BlaSON 1 cruise (1998)
B2KS-xx: cores recovered during BlaSON 2 cruise (2002)
MD04-: cores recovered during ASSEMBLAGE 1 cruise (2004)

References:

Akçar, N. et al., 2009. First results on determination of cosmogenic Cl-36 in limestone from the Yenicekale Complex in the Hittite capital of Hattusha (Turkey). Quaternary Geochronology, 4(6): 533-540.

Aksu, A.E. et al., 2002a. Persistent Holocene outflow from the Black Sea to the eastern Mediterranean contradicts Noah's Flood hypothesis. GSA Today, 12(5): 4-10.

Aksu, A.E., Hiscott, R.N., Yasar, D., Isler, F.I. and Marsh, S., 2002b. Seismic stratigraphy of Late Quaternary deposits from the southwestern Black Sea shelf: evidence for non-catastrophic variations in sea-level during the last ~10000 yr. Marine Geology, 190(1-2): 61-94.

Algan, O. et al., 2001. Stratigraphy of the sediment infill in Bosphorus Strait: water exchange between the Black and Mediterranean Seas during the last glacial-Holocene. Geo-Marine Letters, 20(4): 209-218.

Algan, O. et al., 2002. A high-resolution seismic study in Sakarya Delta and Submarine Canyon, southern Black Sea shelf. Continental Shelf Research, 22(10): 1511-1527.

Aloisi, G., Wallmann, K., Drews, M. and Bohrmann, G., 1992. Multidimensional seismic exploration and its first application results.; 54th meeting and technical exhibition; technical programme and abstracts of papers (oral and poster presentations). Geochemistry, Geophysics, Geosystems, 54: 12-13.

Alpar, B. and Yaltirak, C., 2002. Characteristic features of the North Anatolian Fault in the eastern Marmara region and its tectonic evolution. Marine Geology, 190(1-2): 329-350.

Altinok, Y., Alpar, B., Ozer, N. and Aykurt, H., 2011. Revision of the tsunami catalogue affecting Turkish coasts and surrounding regions. Natural Hazards and Earth System Sciences, 11(2): 273-291.

Armijo, R., Meyer, B., Hubert, A. and Barka, A., 1999. Westward propagation of the North Anatolian fault into the northern Aegean: Timing and kinematics. Geology, 27(3): 267-270.

Armijo, R., Meyer, B., Navarro, S., King, G. and Barka, A., 2002. Asymmetric slip partitioning in the Sea of Marmara pull-apart: a clue to propagation processes of the North Anatolian Fault? Terra Nova, 14: 80-86.

Atalay, I., 1996. Palaeosols as indicators of the climatic changes during Quaternary period in S. Anatolia. Journal of Arid Environments, 32(1): 23-35.

Bahr, A., Arz, H.W., Lamy, F. and Wefer, G., 2006. Late glacial to Holocene paleoenvironmental evolution of the Black Sea, reconstructed with stable oxygen isotope records obtained on ostracod shells. Earth and Planetary Science Letters, 241(3-4): 863-875.

Bahr, A., Lamy, F., Arz, H., Kuhlmann, H. and Wefer, G., 2005. Late glacial to Holocene climate and sedimentation history in the NW Black Sea. Marine Geology, 214(4): 309-322.

Bahr, A. et al., 2008. Abrupt changes of temperature and water chemistry in the late Pleistocene and early Holocene Black Sea. Geochemistry Geophysics Geosystems, 9(Q01004, doi:10.1029/2007GC001683): 1-16.

Bahr, A. et al., 2009. Authigenic carbonate precipitates from the NE Black Sea: a mineralogical, geochemical, and lipid biomarker study. International Journal of Earth Sciences, 98(3): 677-695.

Barka, A., Akyüz, H.S., Cohen, H.A. and Watchorn, F., 2000. Tectonic evolution of the Niksar and Tasova-Erbaa pull-apart basins, North Anatolian Fault Zone: their significance for the motion of the Anatolian block. Tectonophysics, 322(3-4): 243-264.

Beck, C. et al., 2007. Late Quaternary co-seismic sedimentation in the Sea of Marmara's deep basins. Sedimentary Geology, 199(1-2): 65-89.

Berger, A. and Loutre, M.F., 2002. An exceptionally long interglacial ahead ? Science, 297: 1287-1288.

Bouma, A., Coleman, J., Stelting, C. and Kohl, B., 1989. Influence of relative sea level changes on the construction of the Mississippi Fan. Geo-Marine Letters, 9(3): 161-170.

Bouma, A.H., 1962. Sedimentology of some Flysch deposits;: A graphic approach to facies interpretation. Elsevier, Amsterdam, NL, 168 pp.

Bourget, J. et al., 2011. Turbidite system architecture and sedimentary processes along topographically complex slopes: the Makran convergent margin. Sedimentology, 58(2): 376-406.

Bourget, J. et al., 2010. Highstand vs. lowstand turbidite system growth in the Makran active margin: Imprints of high-frequency external controls on sediment delivery mechanisms to deep water systems. Marine Geology, 274(1-4): 187-208.

Çagatay, M.N. et al., 2000. Late Glacial-Holocene palaeoceanography of the Sea of Marmara: timing of connections with the Mediterranean and the Black Seas. Marine Geology, 167: 191-206.

Canals, M. et al., 2004. Slope failure dynamics and impacts from seafloor and shallow sub-seafloor geophysical data: case studies from the COSTA project. Marine Geology, 213(1-4): 9-72.

Chapron, E. et al., 2006. Impact of the 1960 major subduction earthquake in Northern Patagonia (Chile, Argentina). Quaternary International, 158: 58-71.

Chapron, E., Beck, C., Pourchet, M. and Deconinck, J.F., 1999. 1822 earthquake-triggered homogenite in Lake Le Bourget (NW Alps). Terra Nova, 11(2-3): 86-92.

Cifci, G., Dondurur, D. and Ergun, M., 2003. Deep and shallow structures of large pockmarks in the Turkish shelf, eastern Black Sea.; Contributions from the combined 7th international conference on Gas in marine sediments and the NATO advanced research workshop on Seafloor hydrocarbon seeps. Geo-Marine Letters, 23: 311-322.

Cita, M.B., Camerlenghi, A., Kastens Kim, A. and McCoy, F.W., 1984. New findings of Bronze Age homogenites in the Ionian Sea; geodynamic implications for the Mediterranean. Marine Geology, 55(1-2): 47-62.

Cita, M.B., Camerlenghi, A. and Rimoldi, B., 1996. Deep-sea tsunami deposits in the eastern Mediterranean: New evidence and depositional models. Sedimentary Geology, 104(1-4): 155-173.

Clark, J.D., Kenyon, N.H. and Pickering, K.T., 1992. Quantitative-Analysis of the Geometry of Submarine Channels - Implications for the Classification of Submarine Fans. Geology, 20(7): 633-636.

Damuth, J.E., Flood, R.D., Kowsmann, R.O., Belderson, R.H. and Gorini, M.A., 1988. Anatomy and Growth-Pattern of Amazon Deep-Sea Fan as Revealed by Long-Range Side-Scan Sonar (Gloria) and High-Resolution Seismic Studies. Aapg Bulletin-American Association of Petroleum Geologists, 72(8): 885-&.

Degens, E.T. and Ross, D.A., 1974. The Black Sea - Geology, Chemistry and Biology, 20. Amer. Assoc. Petroleum Geol., Tulsa, 633 pp.

Demirbag, E., Gökasan, E., Oktay, F.Y., Simsek, M. and Yüce, H., 1999. The last sea level changes in the Black Sea: evidence from the seismic data. Marine Geology, 157(3-4): 249-265.

Denton, G.H. et al., 2010. The Last Glacial Termination. Science, 328(5986): 1652-1656.

Dondurur, D. and Cifci, G., 2007. Acoustic structure and recent sediment transport processes on the continental slope of Yesilirmak River fan, Eastern Black Sea. Marine Geology, 237(1-2): 37-53.

Dondurur, D. and Cifci, G., 2009. Anomalous Strong Reflections on High Resolution Seismic Data from the Turkish Shelf of the Eastern Black Sea: Possible Indicators of Shallow Hydrogen Sulphide-Rich Gas Hydrate Layers. Turkish Journal of Earth Sciences, 18(2): 299-313.

Droz, L. et al., 2003. Architecture of an active mud-rich turbidite system: The Zaire Fan (Congo-Angola margin southeast Atlantic): Results from ZaiAngo 1 and 2 cruises. Aapg Bulletin, 87(7): 1145-1168.

Droz, L., Rigaut, F., Cochonat, P. and Tofani, R., 1996. Morphology and recent evolution of the Zaire turbidite system (Gulf of Guinea). Geological Society of America Bulletin, 108(3): 253-269.

Ducassou, E. et al., 2007. Multiproxy late quaternary stratigraphy of the Nile deep-sea turbidite system - Towards a chronology of deep-sea terrigeneous systems. Sedimentary Geology, 200(1-2): 1-13.

Duman, M. et al., 2006. Geochemistry and sedimentology of shelf and upper slope sediments of the south-central Black Sea. Marine Geology, 227(1-2): 51-65.

Elmas, A., 2003. Late Cenozoic tectonics and stratigraphy of northwestern Anatolia: the effects of the North Anatolian Fault to the region. International Journal of Earth Sciences, 92(3): 380-396.

Faccenna, C., Bellier, O., Martinod, J., Piromallo, C. and Regard, V., 2006. Slab detachment beneath eastern Anatolia: A possible cause for the formation of the North Anatolian fault. Earth and Planetary Science Letters, 242(1-2): 85-97.

Flerit, F., Armijo, R., King, G. and Meyer, B., 2004. The mechanical interaction between the propagating North Anatolian Fault and the back-arc extension in the Aegean. Earth and Planetary Science Letters, 224(3-4): 347-362.

Flood, R.D. and Damuth, J.E., 1987. Quantitative Characteristics of Sinuous Distributary Channels on the Amazon Deep-Sea Fan. Geological Society of America Bulletin, 98(6): 728-738.

Flood, R.D., Piper, D.J.W. and Klaus, A., 1994. Amazon deep-sea fan. JOIDES Journal, 20(1): 32-34.

Fontugne, M., Guichard, F., Strechie, C. and Lericolais, G., 2009. Reservoir age of the Black Sea waters during anoxic periods Radiocarbon, 51(3): 969-976.

Garziglia, S. et al., 2007. Triggering factors and tsunamigenic potential of a large submarine mass failure on the western Nile margin (Rosetta area, Egypt). Submarine Mass Movements and Their Consequences, 27: 347-355.

Gasse, F. and Fontes, J.-C., 1992. Climatic changes in northwest Africa during the last deglaciation. In: E. Bard and W.S. Wallace (Editors), The Last Deglaciation: Absolute and Radiocarbon Chronologies. Nato ASI Series, Berlin, pp. 295-325.

Gervais, A., Mulder, T., Savoye, B., Migeon, S. and Cremer, M., 2001. Recent processes of levee formation on the Zaire deep-sea fan. Comptes Rendus de l'Academie des Sciences - Series IIA - Earth and Planetary Science, 332(6): 371-378.

Gillet, H., Lericolais, G. and Réhault, J.-P., 2007. Messinian event in the Black Sea: evidence of the erosional surface. Marine Geol., 244(1-4): 142-165.

Giosan, L., 2009. Danube Delta Holds Answers To 'Noah's Flood' Debate. , ScienceDaily.

Giosan, L. et al., 2006. Young Danube delta documents stable Black Sea level since the middle Holocene: Morphodynamic, paleogeographic, and archaeological implications. Geology, 34(9): 757-760.

Giosan, L., Filip, F. and Constatinescu, S., 2009. Was the Black Sea catastrophically flooded in the early Holocene? Quaternary Science Reviews, 28(1-2): 1-6.

Giunta, S., Morigi, C., Negri, A., Guichard, F. and Lericolais, G., 2007. Holocene biostratigraphy and paleoenvironmental changes in the Black Sea based on calcareous nannoplankton. Marine Micropaleontology, 63(1-2): 91-110.

Glenn, C.R. and Arthur, M.A., 1985. Sedimentary and geochemical indicators of productivity and oxygen contents in modern and ancient basins; the Holocene Black Sea as the "type" anoxic basin. Chemical Geology, 48(1-4): 325-354.

Gorur, N. et al., 2001. Is the abrupt drowning of the Black Sea shelf at 7150 yr BP; a myth? Marine Geology, 176(1-4): 65-73.

Guichard, F., Carey, S., Arthur, M.A., Sigurdsson, H. and Arnold, M., 1993. Tephra from the Minoan eruption of Santorini in sediments of the Black Sea. Nature, 363(17): 610-612.

Hickson, T. A., and Lowe, D. R. (2002). Facies architecture of a submarine fan channel-levee complex: The Juniper Ridge Conglomerate, Coalinga, California. Sedimentology 49, 335-362.

Jegou, I., Savoye, B., Pirmez, C. and Droz, L., 2008. Channel-mouth lobe complex of the recent Amazon Fan: The missing piece. Marine Geology, 252(1-2): 62-77.

Jones, G.A. and Gagnon, A.R., 1994. Radiocarbon chronology of Black Sea sediments. Deep Sea Research 1, 41(3): 531-557.

Jones, R.W. and Simmons, M.D., 1997. A review of the stratigraphy of Eastern Parathethys (Oligocene-Holocene), with particular emphasis on the Black Sea. In: A.G. Robinson (Editor), Regional and petroleum geology of the Black Sea and surrounding region. American Association of Petroleum Geologists Bulletin, pp. 39-52.

Kastens, K.A. and Cita, M.B., 1981. Tsunami-Induced Sediment Transport in the Abyssal Mediterranean-Sea. Geological Society of America Bulletin, 92(11): 845-857.

Kenyon, N.H., Amir, A. and Cramp, A., 1995. Geometry of the younger sediment bodies of the Indus Fan. In: K.T. Pickering, R.N. Hiscott, N.H. Kenyon, F. Ricci Lucchi and R.D.A. Smith (Editors), Atlas of Deep Water Environments: Architectural Style in Turbidite Systems. Chapman & Hall, Oxford, pp. 89–93.

Konyukhov, A.I., 1997. The Danube submarine fan: specific features of the structure and sediment accumulation. Lithology and Mineral Resources, 32(3): 197-207.

Kwiecien, O. et al., 2009. North Atlantic control on precipitation pattern in the eastern Mediterranean/Black Sea region during the last glacial. Quaternary Research, 71(3): 375-384.

Kwiecien, O. et al., 2008. Estimated reservoir ages of the Black Sea since the last glacial. Radiocarbon, 50(1): 99-118.

Lamy, F., Arz, H.W., Bond, G.C., Bahr, A. and Pätzold, J., 2006. Multicentennial-scale hydrological changes in the Black Sea and northern Red Sea during the Holocene and the Arctic/North Atlantic Oscillation. Paleoceanography, 21(1): PA1008.

Landmann, G., Reimer, A., Lemcke, G. and Kempe, S., 1996. Dating Late Glacial abrupt climate changes in the 14,570 yr long continuous varve record of Lake Van, Turkey. Palaeogeography, Palaeoclimatology, Palaeoecology, 122(1-4): 107-118.

Lee, S.E., Talling, P.J., Ernst, G.G.J. and Hogg, A.J., 2002. Occurrence and origin of submarine plunge pools at the base of the US continental slope. Marine Geology, 185: 363-377.

Lericolais, G., Bulois, C., Gillet, H. and Guichard, F., 2009. High frequency sea level fluctuations recorded in the Black Sea since the LGM. Global and Planetary Change, 66(1-2): 65-75.

Lericolais, G. et al., 2010. A post Younger Dryas Black Sea regression identified from sequence stratigraphy correlated to core analysis and dating. Quaternary International, 225(2): 199-209.

Lericolais, G. et al., 2011. Assessment of Black Sea water-level fluctuations since the Last Glacial Maximum. In: I. Buynevich, V. Yanko-Hombach, A.S. Gilbert and R.E. Martin (Editors), Geology and Geoarchaeology of the Black Sea Region: Beyond the Flood Hypothesis. The Geological Society of America, Boulder, Colorado, pp. 33–50.

Lericolais, G., Popescu, I., Guichard, F. and Popescu, S.M., 2007a. A Black Sea lowstand at 8500 yr B.P. indicated by a relict coastal dune system at a depth of 90 m below sea level. In: J. Harff,

W.W. Hay and D.M. Tetzlaff (Editors), Coastline Changes: Interrelation of Climate and Geological Processes. GSA Books; Allen Press, Inc., Special Paper 426, pp. 171-188.

Lericolais, G., Popescu, I., Guichard, F., Popescu, S.M. and Manolakakis, L., 2007b. Water-level fluctuations in the Black Sea since the Last Glacial Maximum. In: V. Yanko-Hombach, A.S. Gilbert, N. Panin and P.M. Dolukhanov (Editors), The Black Sea Flood Question: Changes in Coastline, Climate, and Human Settlement. Springer, pp. 437-452.

Lowe, D.R., 1982. Sediment Gravity Flows .2. Depositional Models with Special Reference to the Deposits of High-Density Turbidity Currents. Journal of Sedimentary Petrology, 52(1): 279-298.

Lykousis, V. et al., 2007. Sediment failure processes in active grabens: The Western Gulf of Corinth (Greece). Submarine Mass Movements and Their Consequences, 27: 297-305.

Major, C., Goldstein, S.L., Ryan, W., Piotrowski, A. and Lericolais, G., 2002a. Climate change in the black sea region through termination I from Sr and O isotopes. Geochimica Et Cosmochimica Acta, 66(15A): A476-A476.

Major, C.O. et al., 2006. The co-evolution of Black Sea level and composition through the last deglaciation and its paleoclimatic significance. Quaternary Science Reviews, 25(17-18): 2031-2047.

Major, C.O., Ryan, W.B.F., Lericolais, G. and Hajdas, I., 2002b. Constraints on Black Sea outflow to the Sea of Marmara during the last glacial-interglacial transition. Marine Geology, 190(1-2): 19-34.

Marsset, T., Droz, L., Dennielou, B. and Pichon, E., 2009. Cycles in the Architecture of the Quaternary Zaire Turbidite System: a Possible Link with Climate. External Controls on Deep-Water Depositional Systems(92): 89-106.

Mas, V. et al., 2010. Multiscale spatio-temporal variability of sedimentary deposits in the Var turbidite system (North-Western Mediterranean Sea). Marine Geology, 275(1-4): 37-52.

Maslin, M., Vilela, C., Mikkelsen, N. and Grootes, P., 2005. Causes of catastrophic sediment failures of the Amazon Fan. Quaternary Science Reviews, 24(20-21): 2180-2193.

McClusky, S. et al., 2000. Global Positioning System constraints on plate kinematics and dynamics in the eastern Mediterranean and Caucasus. J. Geophys. Res., 105(B3): 5695-5719.

McHugh, C.M.G. et al., 2006. Submarine earthquake geology along the North Anatolia Fault in the Marmara Sea, Turkey: A model for transform basin sedimentation. Earth and Planetary Science Letters, 248(3-4): 661-684.

Middleton, G.V. and Hampton, M.A., 1973. Sediment gravity flows: Mechanics of flow and deposition. In: G.V. Middleton and A.H. Bouma (Editors), Turbidites and deepwater sedimentation. Pacific section Society of Economic Paleontologists and Mineralogists, Los Angeles, pp. 1-38.

Migeon, S. et al., 2010. Lobe construction and sand/mud segregation by turbidity currents and debris flows on the western Nile deep-sea fan (Eastern Mediterranean). Sedimentary Geology, 229(3): 124-143.

Migeon, S., Weber, O., Faugeres, J.C. and Saint-Paul, J., 1999. SCOPIX: A new X-ray imaging system for care analysis. Geo-Marine Letters, 18(3): 251-255.

Mulder, T. and Alexander, J., 2001. The physical character of subaqueous sedimentary density flows and their deposits. Sedimentology, 48(2): 269-300.

Murray, J.W. et al., 1989. Unexpected changes in the oxic/ anoxic interface in the Black Sea. Nature (London), 338(6214): Pages 411-413.

Myers, P.G., Wielki, C., Goldstein, S.B. and Rohling, E.J., 2003. Hydraulic calculations of postglacial connections between the Mediterranean and the Black Sea. Marine Geology, 201(4): 253-267.

Nikishin, A.M., Korotaev, M.V., Ershov, A.V. and Brunet, M.-F., 2003. The Black Sea basin: tectonic history and Neogene-Quaternary rapid subsidence modelling. Sedimentary Geology, 156(1-4): 149-168.

Nisbet, E.G. and Piper, D.J.W., 1998. Giant submarine landslides. Nature, 392(6674): 329-330.

Normark, W.R., Damuth, J.E. and Group, t.L.S., 1997. Sedimentary facies and associated depositional elements of the Amazon fan. In: R.D. Flood, D.J.W. Piper, A. Klaus and L.C. Peterson (Editors), Proceedings of the Ocean Drilling Project, Scientific Results, Austin, Tx, pp. 611-651.

Pelinovsky, E., 1999. Preliminary estimates of tsunami danger for the northern part of the Black Sea. Physics and Chemistry of the Earth Part a-Solid Earth and Geodesy, 24(2): 175-178.

Piper, D.J.W. and Savoye, B., 1993. Processes of Late Quaternary Turbidity-Current Flow and Deposition on the Var Deep-Sea Fan, North-West Mediterranean-Sea. Sedimentology, 40(3): 557-582.

Pondard, N., Armijo, R., King, G.C.P., Meyer, B. and Flerit, F., 2007. Fault interactions in the Sea of Marmara pull-apart (North Anatolian Fault): earthquake clustering and propagating earthquake sequences. Geophysical Journal International, 171(3): 1185-1197.

Popescu, I., 2002. Analyse des processus sédimentaires récents dans l'éventail profond du Danube (mer Noire). PhD Thesis, Université de Bretagne Occidentale-Université de Bucarest, Brest, 282 pp.

Popescu, I. et al., 2006. Multiple bottom-simulating reflections in the Black Sea: Potential proxies of past climate conditions. Marine Geology, 227(3-4): 163-176.

Popescu, I. et al., 2004. The Danube Submarine Canyon (Black Sea): morphology and sedimentary processes. Marine Geol., 206(1-4): 249-265.

Popescu, I., Lericolais, G., Panin, N., Wong, H.K. and Droz, L., 2001. Late Quaternary channel avulsions on the Danube deep-sea fan. Marine Geology, 179(1-2): 25-37.

Rangin, C., Bader, A.G., Pascal, G., Ecevitoglu, B. and Gorur, N., 2002. Deep structure of the Mid Black Sea High (offshore Turkey) imaged by multi-channel seismic survey (BLACKSIS cruise),. Marine Geology, 182(3-4): 265-278.

Reeder, M., Rothwell, R.G., Stow, D.A.V., Kahler, G. and Kenyon, N.H., 1998. Turbidite flux, architecture and chemostratigraphic of the Herodotus Basin, Levantine Sea, SE Mediterranean. In: M.S. Stocker, D. Evans and A. Cramp (Editors), Geological Processes on Continental Margins. Geol. Soc, London, Spec. Publ. , London, pp. 19–41.

Reimer, P.J. et al., 2009. Intcal09 and Marine09 Radiocarbon Age Calibration Curves, 0-50,000 Years Cal Bp. Radiocarbon, 51(4): 1111-1150.

Richards, M.P., Bowman, M. and Reading, H.G., 1998. Submarine-fan systems I: characterization and stratigraphic prediction. Marine and Petroleum Geology, 15: 689-717.

Robinson, A.G., 1997. Regional and Petroleum Geology of the Black Sea and Surrounding Region, Memoir 68. American Association of Petroleum Geologists, Tulsa, USA.

Robinson, A.G., Rudata, J.H., Banksa, C.J. and Wilesa, R.L.F., 1996. Petroleum geology of the Black Sea. Marine and Petroleum Geology, 13(2): 195-223.

Robinson, A.G., Spadini, G., Cloetingh, S. and Rudat, J., 1995. Stratigraphic evolution of the Black Sea: inferences from basin modelling. Marine and Petroleum Geology, 12(8): 821-835.

Ross, D.A., 1978a. Black Sea Stratigraphy. In: D.A. Ross and Y.P. Neprochnov (Editors), Initial Rep. Deep Sea Drill. Proj. US Govt. Print. Office, Washington, DC, pp. 17-26.

Ross, D.A. (Editor), 1978b. Summary of results of Black Sea Drilling. Initial Rep. Deep Sea Drill. Proj., 42. US Govt. Print. Office, Washington, DC, 1149-1178 pp.

Ross, D.A. and Degens, E.T., 1974. Recent sediments of the Black Sea. In: E.T. Degens and D.A. Ross (Editors), The Black Sea - Geology, Chemistry and Biology. Amer. Assoc. Petrol. Geol., Tulsa, pp. 183-199.

Ross, D.A. and Neprochnov, Y.P. (Editors), 1978. Initial Reports of the Deep Sea Drilling Project. Initial Rep. Deep Sea Drill. Proj., 42, part 2. US Govt. Print. Office, Washington, DC, 1178 pp.

Ross, D.A. et al., 1978. Initial Reports of the Deep Sea Drilling Project. Summary of results of Black Sea Drilling., 42, part 2. US Govt. Print. Office, Washington DC (USA), 1244 pp.

Rotaru, A., 2010. Geoenvironmental Issues Concerning the Black Sea Basin. International Journal of Energy and Environment, 4(4): 131-138.

Rothwell, R.G. et al., 2000. Low sea-level stand emplacement of megaturbidites in the western and eastern Mediterranean Sea. Sedimentary Geology, 135(1-4): 75-88.

Ryan, W.B.F., 2007. Status of the Black Sea flood hypothesis. In: V. Yanko-Hombach, A.S. Gilbert, N. Panin and P.M. Dolukhanov (Editors), The Black Sea Flood Question: Changes in Coastline, Climate, and Human Settlement, pp. 63-88.

Ryan, W.B.F., Major, C.O., Lericolais, G. and Goldstein, S.L., 2003. Catastrophic Flooding of the Black Sea. Annu. Rev. Earth Planet. Sci., 31(1): 525-554.

Ryan, W.B.F. et al., 1997. An abrupt drowning of the Black Sea shelf. Marine Geology, 138(1-2): 119-126.

Savoye, B. et al., 2000a. Structure and recent evolution of the Zaire deep-sea fan: preliminary results of the ZaiAngo 1 & 2 cruises (Angola-Congo margin). Structure et evolution recente de l'eventail turbiditique du Zaire : premiers resultats scientifiques des missions d'exploration Zaiango1 & 2 (marge Congo-Angola). Comptes Rendus de l'Academie des Sciences - Series IIA - Earth and Planetary Science, 331(3): 211-220.

Savoye, B. et al., 2000b. Structure and recent evolution of the Zaire deep-sea fan: preliminary results of the ZaiAngo 1 & 2 cruises (Angola-Congo margin). Comptes Rendus De L Academie Des Sciences Serie Ii Fascicule a-Sciences De La Terre Et Des Planetes, 331(3): 211-220.

Shackleton, N.J., 1987. Oxygen isotopes, ice volume and sea level. Quaternary Science Reviews, 6: 183-190.

Shanmugam, G., 2002. Ten turbidite myths. Earth-Science Reviews, 58(3-4): 311-341.

Siani, G. et al., 2000. Radiocarbon Reservoir Ages in the Mediterranean Sea and Black Sea. Radiocarbon, 42(2): 271-280.

Soulet, G. et al., 2010. Glacial hydrologic conditions in the Black Sea reconstructed using geochemical pore water profiles. Earth and Planetary Science Letters, 296(1-2): 57-66.

Soulet, G., Ménot, G., Lericolais, G. and Bard, E., 2011a. A revised calendar age for the last reconnection of the Black Sea to the global ocean. Quaternary Science Reviews, 30: 1019-1026.

Soulet, G., Ménot, G., Garreta, V., Rostek, F., Zaragosi, S., Lericolais, G., and Bard, E., 2011b. Black Sea "Lake" reservoir age evolution since the Last Glacial -- Hydrologic and climatic implications. Earth and Planetary Science Letters 308, 245-258.

Stanley, D.J., 1983. Mud Carrying Turbidity Currents on the Slope Resulting in Unifites on Basin Plains. Journal of the Geological Society, 140(NOV): 978-978.

Stein, R.S., Barka, A.A. and Dieterich, J.H., 1997. Progressive failure on the North Anatolian fault since 1939 by earthquake stress triggering. Geophysical Journal International, 128(3): 594-604.

Strechie, C. et al., 2002. Magnetic minerals as indicators of major environmental change in holocene black sea sediments: preliminary results. Physics and Chemistry of the Earth, Parts A/B/C, 27(25-31): 1363-1370.

Stuiver, M. and Reimer, P.J., 1993. Extended C-14 Data-Base and Revised Calib 3.0 C-14 Age Calibration Program. Radiocarbon, 35(1): 215-230.

Talling, P.J., Amy, L.A. and Wynn, R.B., 2007. New insight into the evolution of large-volume turbidity currents: comparison of turbidite shape and previous modelling results. Sedimentology, 54(4): 737-769.

Tekiroglu, S.E., Ediger, V., Yemenicioglu, S., Kapur, S. and Akca, E., 2001. The experimental analysis on the Late Quaternary deposits of the Black Sea - (Analyse de sediments holocenes de la Mer Noire). Oceanologica Acta, 24(1): 51-67.

Trincardi, F., Verdicchio, G. and Miserocchi, S., 2007. Seafloor evidence for the interaction between cascading and along-slope bottom water masses. Journal of Geophysical Research-Earth Surface, 112(F3).

Tripsanas, E.K., Bryant, W.R. and Phaneuf, B.A., 2004. Depositional processes of uniform mud deposits (unifites), Hedberg Basin, northwest Gulf of Mexico: New perspectives. Aapg Bulletin, 88(6): 825-840.

Tugolesov, D.A., Gorshkov, A.S., Meysner, L.B., Solov'yev, V.V. and Khakhalev, Y.M., 1985. The tectonics of the Black Sea trough. Geotectonics 19 (6): 435-445.

Wick, L., Lemcke, G. and Sturm, M., 2003. Evidence of Lateglacial and Holocene climatic change and human impact in eastern Anatolia: high-resolution pollen, charcoal, isotopic and geochemical records from the laminated sediments of Lake Van, Turkey. Holocene, 13(5): 665-675.

Winguth, C. et al., 2000. Upper Quaternary water level history and sedimentation in the northwestern Black Sea. Marine Geology, 167(1-2): 127–146.

Wong, H.K., Panin, N., Dinu, C., Georgescu, P. and Rahn, C., 1994. Morphology and post-Chaudian (Late Pleistocene) evolution of the submarine Danube fan complex. Terra Nova, 6: 502-511.

Wong, H.K. et al., 1997. The Danube and Dniepr fans, morphostructure and evolution. GeoEcoMarina, 2: 77-102.

Wynn, R.B. and Stow, D.A.V., 2002. Classification and characterisation of deep-water sediment waves. Marine Geology, 192(1-3): 7-22.

Zahno, C., Akçar, N., Yavuz, V., Kubik, P.W. and Schluchter, C., 2010. Chronology of Late Pleistocene glacier variations at the Uludag Mountain, NW Turkey. Quaternary Science Reviews, 29(9-10): 1173-1187.

Zaragosi, S. et al., 2000. Physiography and recent sediment distribution of the Celtic Deep-Sea Fan, Bay of Biscay. Marine Geology, 169: 207-237.

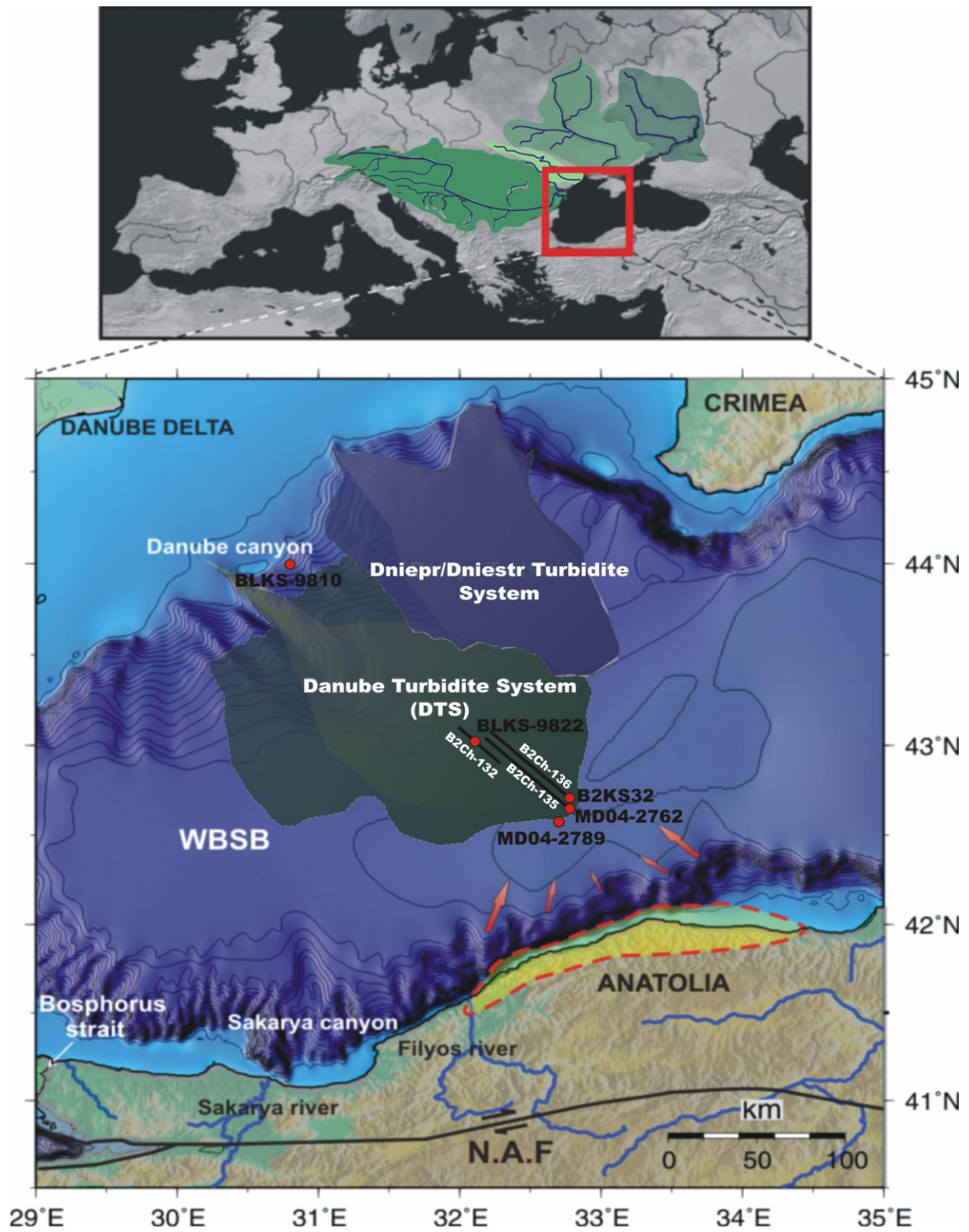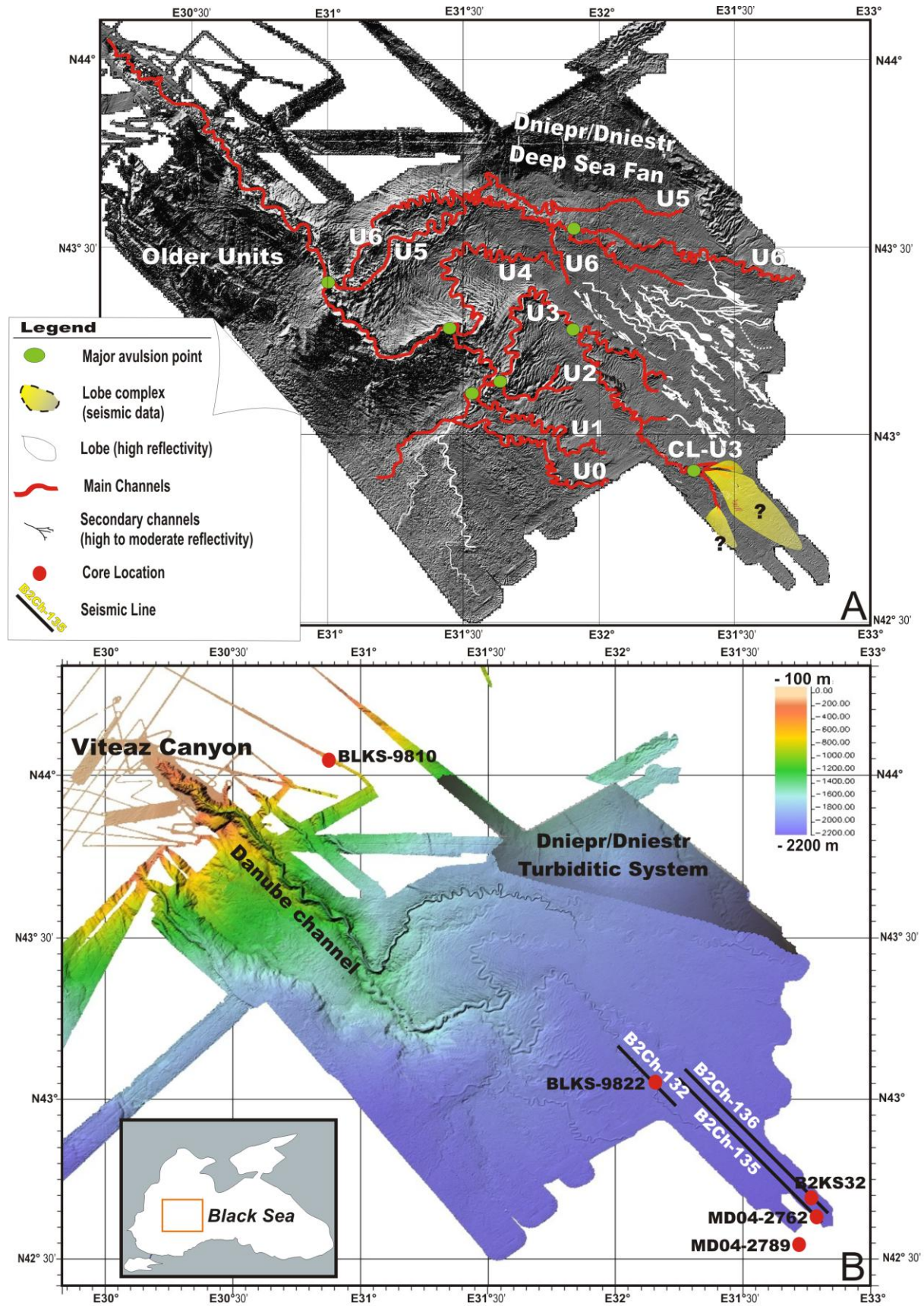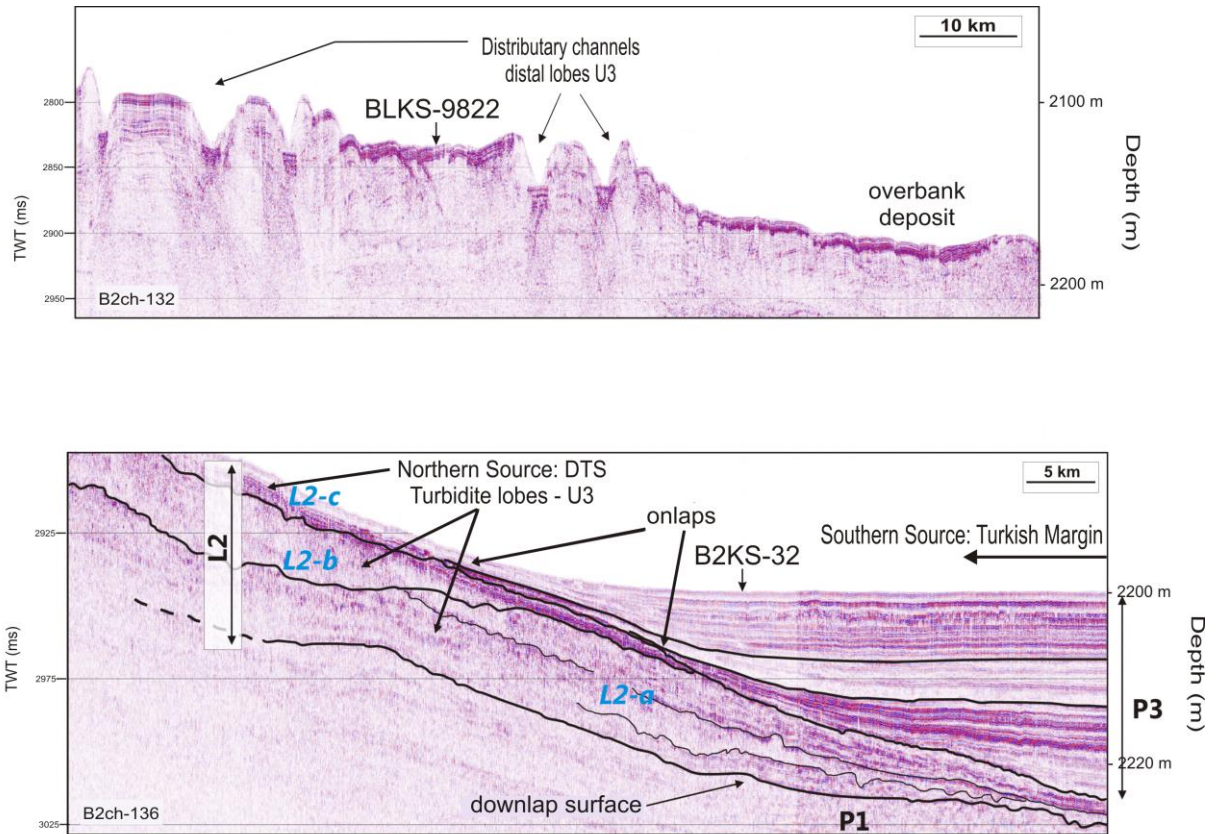Zonenshain, L.P. and Pichon, X., 1986. Deep basins of the Black Sea and Caspian Sea as remnants of
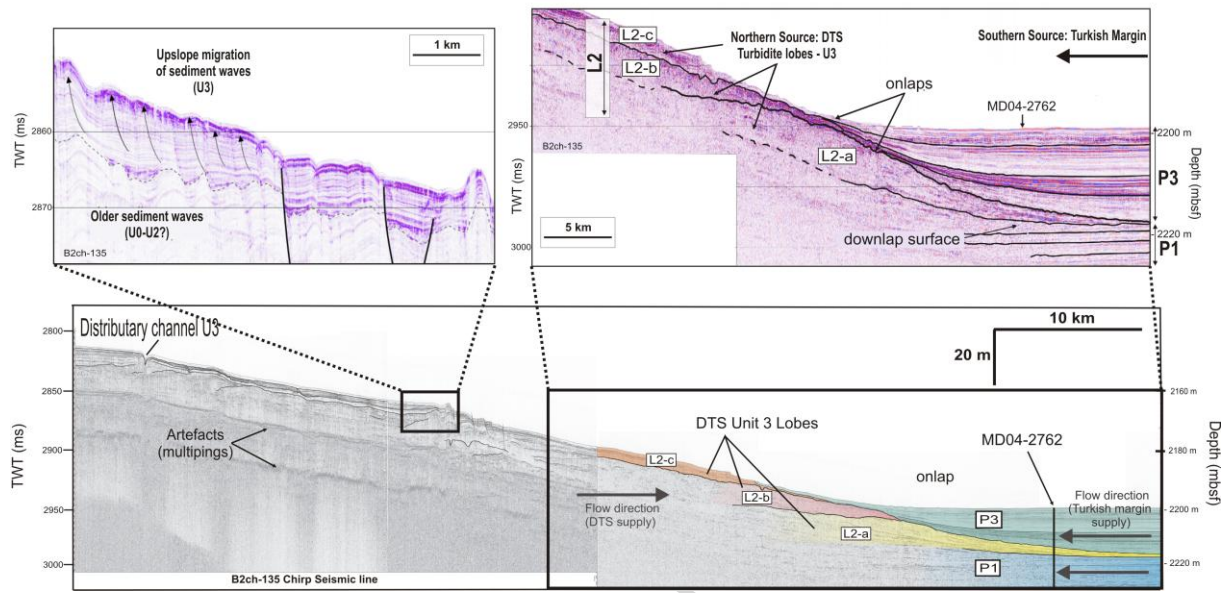
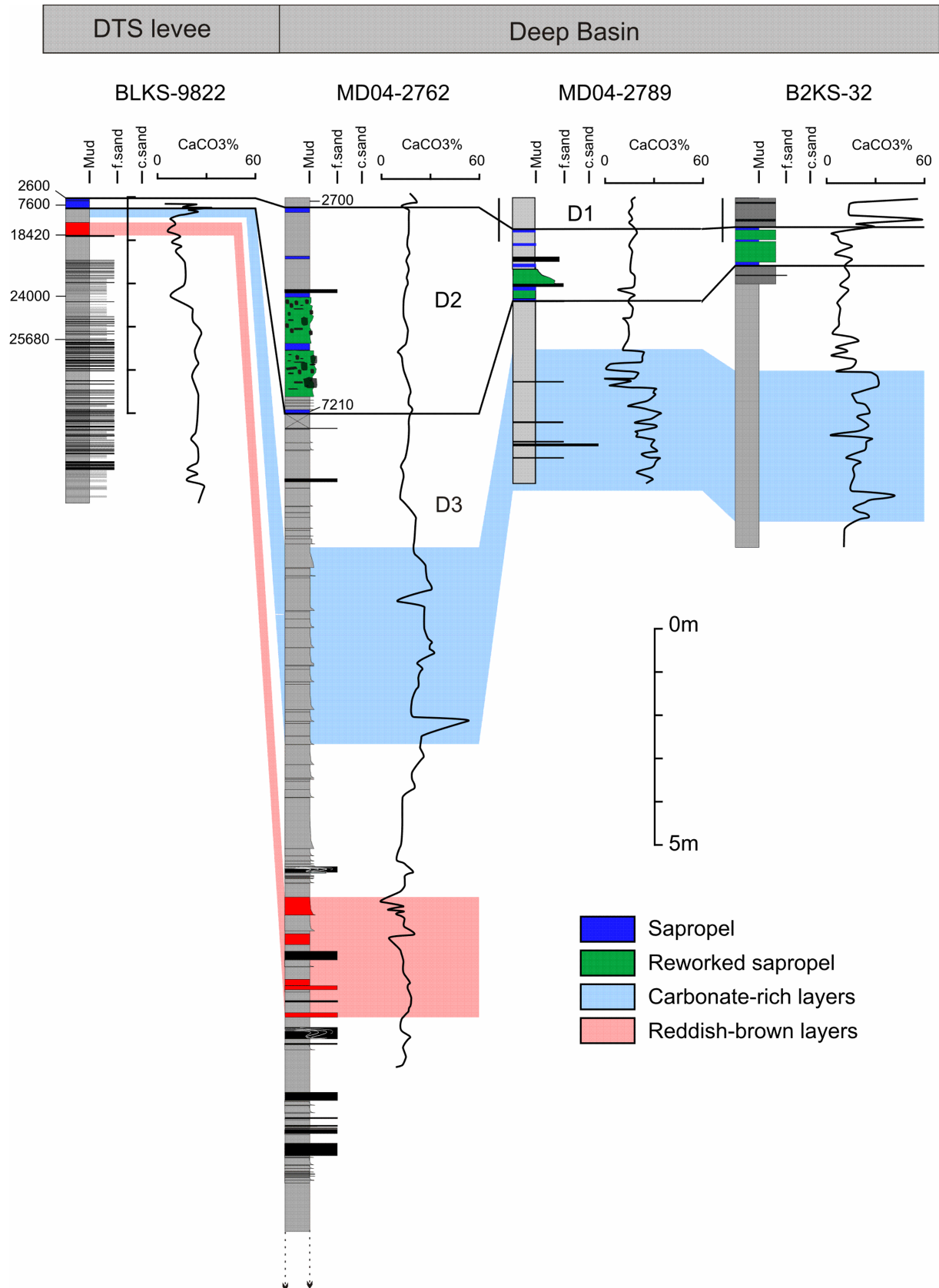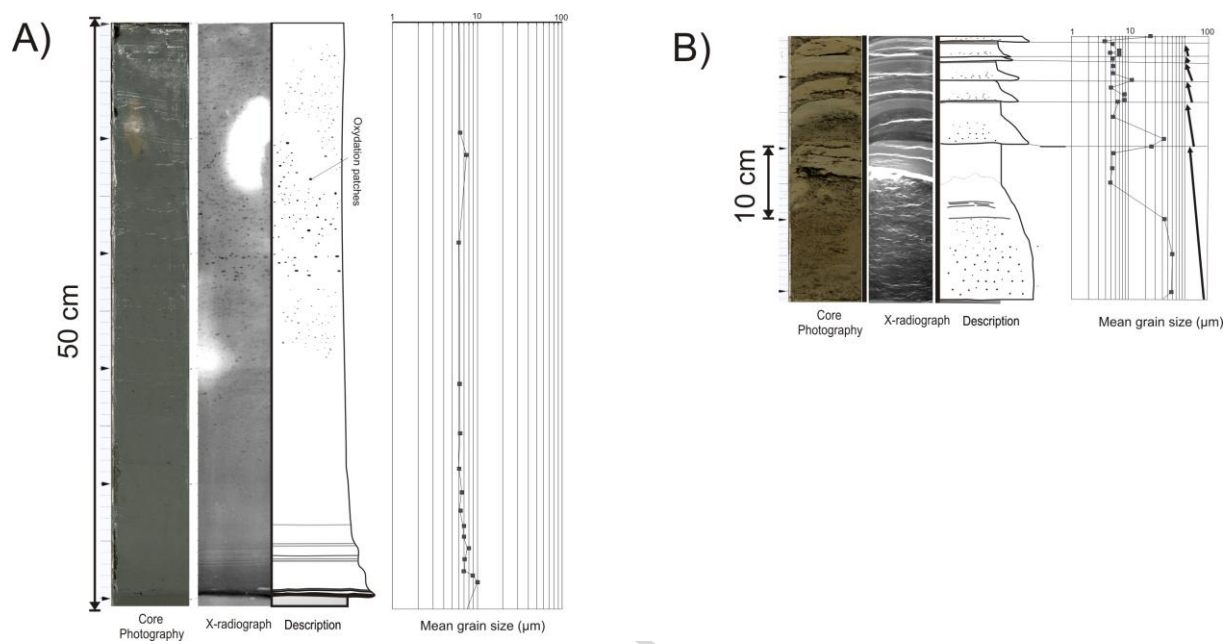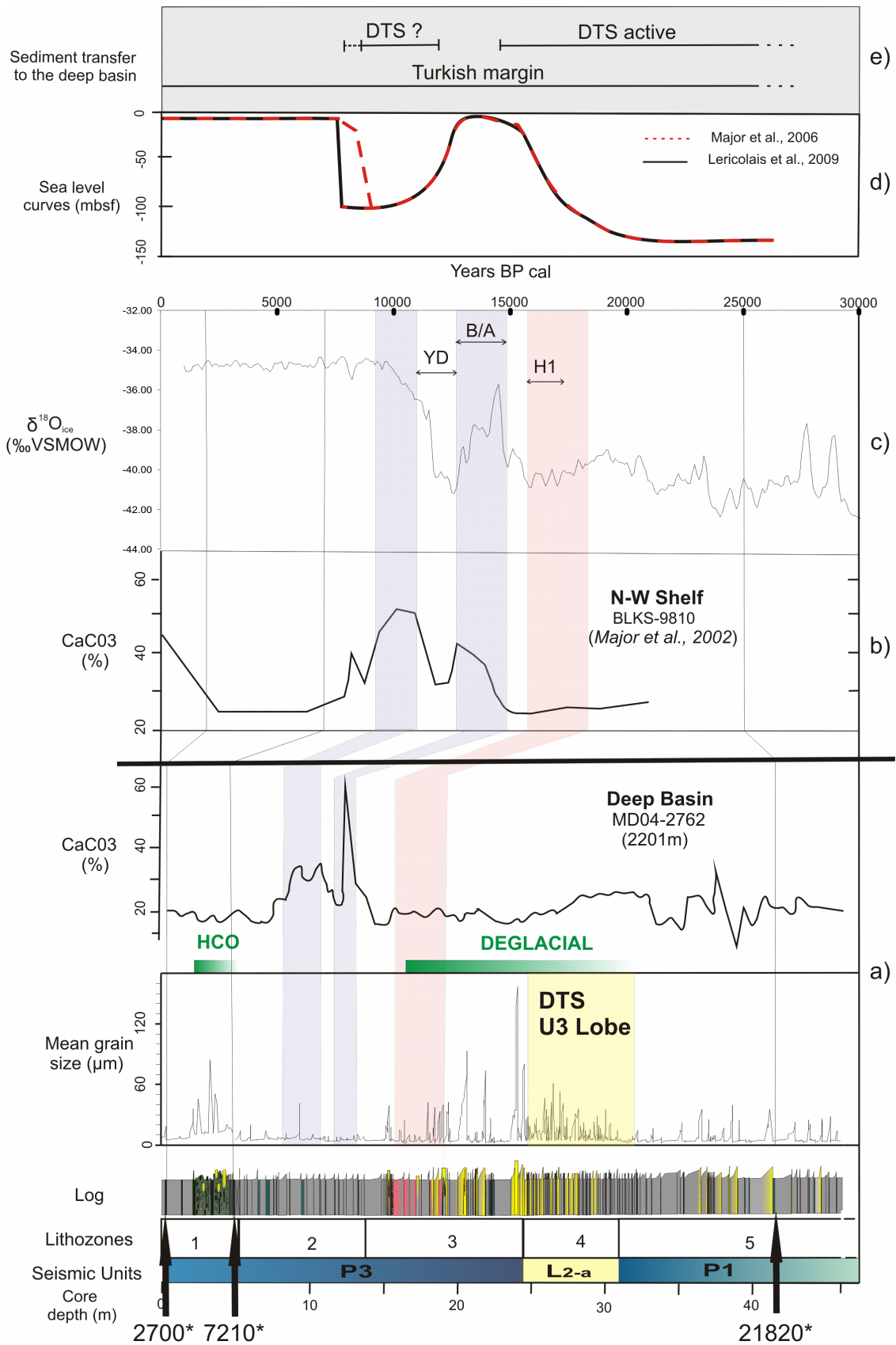Fig. 1

Fig. 2

Fig. 3

Fig. 4

Fig. 5

Fig. 6

Fig. 7

Fig. 8

Late Quaternary deep-sea sedimentation in the western Black Sea: new insights from recent coring and seismic data in the deep basin.

Highlights

G. Lericolais, J. Bourget, I. Popescu, P. Jermannaud, T. Mulder; S. Jorry; N. Panin

Only few recent studies have focused on the deep-sea morphology and gravity sedimentation in the western Black Sea basin, where the main depositional feature is the Danube submarine fan.

This publication presents results obtained from oceanographic surveys in the Black Sea in 1998, 2002 and 2004 carried out in the framework of French-Romanian joint project and the European ASSEMBLAGE (EVK3-CT-2002-00090) project have collected a large amount of data (Multibeam echosounder data, Chirp seismic, Kullenberg and Calypso cores).

The results of these studies were integrated in an ESF SourceSink project and they are based on new insights from recent coring and seismic data recovered at the boundary of influence of both the distal part of the Danube turbiditic system and the Turkish margin.

This dataset provide a good record of changes in the sedimentary supply and climatic-eustatic changes in the surrounding Black Sea since the last 25 ka. Based on this study, we demonstrate that the deep basin deposits bear the record of the Late Quaternary paleoenvironmental changes and that the western Black Sea basin constitutes an asymmetric subsident basin bordered by a northern passive margin with confined mid-size, mud-rich turbiditic systems, and a southern turbiditic ramp margin, tectonically active.